

## The characteristics of millisecond pulsar emission: I. Spectra, pulse shapes and the beaming fraction

Michael Kramer<sup>1</sup>, Kiriaki M. Xilouris<sup>2</sup>, Duncan R. Lorimer<sup>1</sup>, Oleg Doroshenko<sup>1</sup>, Axel Jessner<sup>1</sup>,  
Richard Wielebinski<sup>1</sup>, Alexander Wolszczan<sup>3</sup>, Fernando Camilo<sup>4</sup>

### ABSTRACT

The extreme physical conditions in millisecond pulsar magnetospheres as well as their different evolutionary history compared to “normal pulsars” raise the question as to whether these objects also differ in their radio emission properties. We have monitored a large sample of millisecond pulsars for a period of three years using the 100-m Effelsberg radio telescope in order to compare the radio emission properties of these two pulsar populations. Our sample comprises a homogeneous data set of very high quality.

With some notable exceptions, our findings suggest that the two groups of objects share many common properties. A comparison of the spectral indices between samples of normal and millisecond pulsars demonstrates that millisecond pulsar spectra are not significantly different from those of normal pulsars. This is contrary to what has previously been thought. There is evidence, however, that millisecond pulsars are slightly less luminous and less efficient radio emitters compared to normal pulsars. We confirm recent suggestions that a diversity exists among the luminosities of millisecond pulsars with the isolated millisecond pulsars being less luminous than the binary millisecond pulsars, implying an influence of the different evolutionary history on the emission properties. There are indications that old millisecond pulsars exhibit somewhat flatter spectra than the presumably younger ones.

Contrary to common belief, we present evidence that the millisecond pulsar profiles are only marginally more complex than those found among the normal pulsar population. Moreover, the development of the profiles with frequency is rather slow, suggesting very compact magnetospheres. The profile development seems to anti-correlate with the companion mass and the spin period, again suggesting that the amount of mass transfer in a binary system might directly influence the emission properties. The angular radius of radio beams of millisecond pulsars does not follow the scaling predicted from

---

<sup>1</sup>Max-Planck-Institut für Radioastronomie, Auf dem Hügel 69, 53121 Bonn, Germany

<sup>2</sup>National Astronomy and Ionosphere Center, Arecibo Observatory, P.O. Box 995, Arecibo, PR 00613, USA

<sup>3</sup>Department of Astronomy and Astrophysics, Penn State University, University Park, PA 16802, USA

<sup>4</sup>Nuffield Radio Astronomy Laboratories, Jodrell Bank, Macclesfield, Cheshire SK11 9DL, England; Marie Curie Fellow

a canonical pulsar model which is applicable for normal pulsars. Instead they are systematically smaller, supporting the concept of a critical rotational period below which such a scaling ceases to exist. The smaller inferred luminosity and narrower emission beams will need to be considered in future calculations of the birth-rate of the Galactic population.

*Subject headings:* Pulsars: millisecond pulsars – normal pulsars – sub-millisecond pulsars – emission mechanism – birth-rates

## 1. Introduction

At the time of the discovery of the first millisecond pulsar B1937+21 by Backer et al. (1982) around 350 pulsars were known. While most of these had periods around one second, the period of PSR B1937+21 was a mere 1.6 ms, immediately raising the question in what respect such objects differ from long period pulsars. Like the original binary pulsar, B1913+16 with a period of 59 ms, it was proposed that millisecond pulsars originate in binary systems in which a slowly rotating neutron star gets spun-up by mass transfer from the binary companion (Alpar et al. 1982). This idea is supported by the fact that 80% of all millisecond pulsars found in the Galactic plane are members of binary systems. These binary systems can be divided into three groups, depending on the mass of the companion star (Camilo 1996), *viz.*: low-mass (presumably Helium) white dwarfs, high-mass (presumably Carbon-Oxygen) white dwarfs and other neutron stars. The progenitors are therefore thought to be either low-mass or high-mass X-ray binary systems. It seems fairly well established that millisecond pulsars are recycled pulsars originating from interacting binary systems. As the exact definition of “millisecond pulsars” in terms of period is somewhat arbitrary, it seems reasonable to treat all recycled pulsars as one class, referring to them as MSPs in the following.

Since the special evolutionary history distinguishes MSPs from long period pulsars, it is consequently interesting to compare the observed properties of these two classes of objects. The most obvious difference between the two classes is, of course, the observed range of pulse periods. The average period of slowly rotating pulsars (hereafter referred to as ‘normal’ pulsars) is about 0.7 s. Rapidly rotating pulsars exhibit pulse periods between 1.5 ms and about 60 ms. The period derivatives of MSPs are a few orders of magnitude smaller than those of normal pulsars, i.e., of the order of  $10^{-19}$  or smaller compared to typically  $10^{-15}$  for normal pulsars. The derived characteristic ages,  $\tau = P/2\dot{P}$ , are of the order of  $10^9$  yr for MSPs and thus much larger than  $10^6$  yr typically found for normal pulsars, indicating that MSPs represent an old population. Similarly, calculating the surface magnetic field for MSPs, i.e.,  $B = 3.2 \cdot 10^{19} \sqrt{P\dot{P}}$  Gauss if  $P$  is measured in seconds (Manchester & Taylor 1977), we find typically values of the order of only  $10^8$  to  $10^9$  Gauss. An outstanding mystery is how the magnetic field decreases from  $10^{12}$  Gauss for normal pulsars by

three to four orders of magnitude during or after the recycling process (e.g., Bhattacharya & van den Heuvel 1991; Phinney & Kulkarni 1994).

For normal pulsars, the magnetic field seems to maintain a dipolar form even at distances of a few stellar radii above the neutron star surface (Phillips 1992; Xilouris et al. 1996; Kramer et al. 1997). For MSPs it has been suggested that flux expulsion as a result of a pre-recycling spin-down (e.g., Srinivasan et al. 1990; Jahan Miri & Bhattacharya 1994), or the spin-up process of accreting mass on the neutron star surface itself (e.g., Romani 1990; Geppert & Urpin 1996) could not only reduce the magnetic field strength, but could also have an impact on the magnetic field structure by disturbing the previously present dipolar field. Moreover, near the surface of MSPs, magnetic multipoles might be present (cf. Ruderman 1991; Arons 1993) which could increase the actual magnetic field strength over the  $10^8$  Gauss inferred from the spin down rates which are dominated by the field structure near the light cylinder (cf. Krolik 1991).

Despite these differences in the observational properties of MSPs and normal pulsars, it is often believed that the emission mechanism responsible for the observed radio emission is the same for both types of pulsars (e.g., Manchester 1992; Gil & Krawczyk 1997). However, there has been no systematic comparison of the emission properties of MSPs and normal pulsars. In a series of papers, we focus on this question which also constrains models of the emission mechanism of normal pulsars. If the same emission theory applies for normal pulsars and MSPs, it implies that the responsible radiation process has to work over three to four orders of magnitude in spin period and magnetic field, ruling out models which depend very much on these parameters (see Melrose 1992). In fact, even if the emission process turns out to be the same for MSPs and normal pulsars, the special evolutionary history of MSPs can be expected to have a certain impact on the observed emission properties, so that it is important to separate such possible effects.

In the past, relatively little work has been done to compare spectral properties of MSPs and normal pulsars. This was primarily due to the small size of the sample — only 5 MSPs were known in the Galactic disk prior to 1990. The first careful study of MSP spectra was presented by Foster, Fairhead, & Backer (1991), obtaining multi-frequency flux densities for four objects. Recently, large-area surveys at Parkes, Arecibo, Jodrell Bank and Green Bank have been very successful at finding MSPs and, as a result, over 35 are presently known in the Galactic disk. Lorimer et al. (1995b) collected data for 20 MSPs mainly from the literature and compared them with a sample of normal pulsars, while Bailes et al. (1997) compared the luminosities of isolated and binary MSPs. Navarro & Manchester (1996) presented high-quality data for PSR J0437–4715 and demonstrated that MSP profiles can exhibit an unusually large number of components. As pointed out by Backer (1995), a systematic study of the complexity of MSP profiles however has not yet been undertaken. Similarly, due to the limited resolution in many of the previously published MSP profiles, it has been difficult to investigate the general width of MSP profiles, which is necessary when making inferences about the intrinsic size of the emission beam.

In this paper we present data obtained over three years during a monitoring project of MSPs

at 1400 MHz. We used the Effelsberg 100-m radio telescope of the MPIfR and could thus observe all MSPs with declinations greater than  $-29^\circ$  which were strong enough to obtain data of high quality. As a result, we present profiles of 27 MSPs, of which 24 are located in the Galactic disk, so that our sample contains about 60% of all known Galactic disk MSPs. Most of the profiles are of high quality both in signal-to-noise ratio and time resolution, thus allowing much more detailed studies than previously possible. Therefore, in this and subsequent papers (Xilouris et al. 1998a, hereafter paper II; Xilouris, Kramer & von Hoensbroech 1998b, hereafter paper III; Kramer et al. 1998) we investigate the largest homogeneous sample of MSP data studied to date.

We investigate the spectra and observed luminosity distributions of MSPs. Attempting to infer the structure and size of the emission beam, we then study the profile properties of MSPs. Searching for possible differences, a detailed comparison with the properties of normal pulsars is made (cf., Manchester & Taylor 1977; Rankin 1983; Lyne & Manchester 1988; Taylor, Manchester, & Lyne 1993; Malofeev et al. 1994; Lorimer et al. 1995a; Seiradakis et al. 1995, Xilouris et al. 1996, Kijak et al. 1997b). This study is complemented by the subsequent papers mentioned above to investigate the polarisation properties of MSPs, the stability of their pulse profiles and the emission height of their radio emission.

## 2. Instrumental set-up and data reduction

The data presented here were obtained during a project which was initiated to obtain pulse time-of-arrival measurements for a number of MSPs during the upgrade of the Arecibo telescope<sup>5</sup> (Wolszczan 1996, Kramer et al. 1996). Since April 1994 we have made regular observations using the 100-m radio telescope in Effelsberg near Bonn. In order to study the polarisation characteristics, all four Stokes parameters were recorded.

We used a highly sensitive 1.4 GHz HEMT receiver installed in the prime focus of the telescope, which is tunable between 1.3 GHz and 1.7 GHz. The set noise temperature of this system is 25 K at median elevations. The antenna gain at these frequencies is 1.5 K/Jy, independent of elevation. We obtained left-hand (LHC  $\equiv A$ ) and right-hand (RHC  $\equiv B$ ) circularly polarised signals across a 40 MHz bandwidth usually centered at 1.41 GHz, but sometimes also tuned to 1.71 GHz. The LHC and RHC signals were mixed down to an intermediate frequency of 150 MHz and fed into a passive (‘adding’) polarimeter providing the complex (undetected) outputs of  $A$ ,  $B$ ,  $A - B$  and  $A - iB$  (for a detailed description of this polarimeter and its calibration see Hoensbroech & Xilouris 1997b). Each output was then split into 60 contiguous channels, each of 666 kHz bandwidth, by four  $60 \times 0.666 = 40$  MHz filter banks. The individually detected filter outputs were delayed according to a pre-calculated delay time of the signals caused by dispersion due to the interstellar medium. Finally, the filter outputs were added on-line and these incoherently de-dispersed signals

---

<sup>5</sup>The Arecibo telescope is operated by Cornell University for the National Science Foundation.

were transferred to the Effelsberg Pulsar Observing System (EPOS) backend.

All four data streams could be sampled by the backend with a maximum resolution of 0.2  $\mu\text{s}$ . However, the pulse period was typically divided into 1024 phase bins. The data were folded according to the computed topocentric pulse period which was updated every five seconds. Until the beginning of 1995 the topocentric period was calculated using TEMPO (Taylor & Weisberg 1989), while later on we used TIMAPR developed by Doroshenko & Kopeikin (1995) for computational convenience. A sub-integration of 15 s was finally transferred to disk for off-line reduction.

In order to monitor the gain stability and polarisation characteristics of EPOS, we performed regular calibration measurements using a switchable noise diode. The signal from this noise diode was injected into the waveguide following the antenna horn and was itself compared to the flux density of known continuum calibrators (Ott et al. 1994) during regularly performed pointing observations. Switching on the noise diode regularly after observations of pulsars allowed us to monitor gain differences in LHC and RHC signal paths and to calibrate the pulse energies by comparing these to the noise diode output. Using this reliable method, we obtained a large number of flux density measurements presented in the following section.

### 3. Millisecond pulsar flux densities

In Table 1 we present the results of flux density measurements for 23 pulsars. These measurements were performed repeatedly at 1.41 and 1.71 GHz, and therefore we quote an effective frequency  $\nu_{\text{eff}}$  representing the weighted mean of the centre frequencies used. The error introduced by this procedure is at most 6% (for a steep spectral index of  $-3$ ) and thus *is* much smaller than the uncertainties due to interstellar scintillation. In order to give an impression about the amplitude of any remaining uncertainties due to scintillation, we additionally quote the median of the measured flux densities which can be directly compared to the mean value.

In the following we compare the spectra and luminosities of MSPs and normal pulsars. As we will see, one has to take into account that the sample of MSPs was solely discovered during low frequency surveys, which favoured nearby MSPs due to severe dispersion and scattering limitations. In contrast, the sample of normal pulsars includes a large number of sources found in the previous high frequency surveys by Johnston et al. (1992) and Clifton et al. (1992), which in turn favoured flat spectrum, high luminosity sources (Lorimer et al. 1995b). In order to construct a more homogeneous set of sources which can then be compared, we can restrict the studied samples to those pulsars whose distance is not larger than 1.5 kpc, since we can reasonably assume that for a comparison of normal pulsars and MSPs the population of MSPs has been sufficiently sampled out to this distance (Lyne et al. 1998). Additionally, it will be useful to compare the results obtained for this set of data with those of an analysis of MSPs and normal pulsars detected in a single survey. Evidently, the recent Parkes 436 MHz southern sky survey (Manchester et al. 1996; Lyne et al. 1998) provides such a homogeneous sample to verify our results.

### 3.1. Spectra of MSPs

Using the flux densities which we have measured at 1.4/1.7 GHz presented in Table 1, we have used power law fits to calculate spectral indices based on our flux densities and those published for lower frequencies. Corresponding references and resulting spectral indices are given in Table 1. We also included data presented by Foster et al. (1991), and the recent observations of four MSPs (J1022+1001, J1713+0747, B1855+09 and J2145–0750) at 4.85 GHz by Kijak et al. (1997a). If estimated uncertainties for flux densities found in the literature were not specified, we assumed a typical error of at least 30% due to the expected severe scintillation effects. In cases where we believe that scintillation imposes an even larger uncertainty, we accounted for this effect by increasing the estimated error. Additionally, for those pulsars which are not included in our sample but discussed in the literature, we derived spectral indices for 11 further MSPs located in the Galactic disk (second part of Table 1). Our subsequent analysis does not include PSRs J2019+2425 and J2322+2057, although we present pulse profiles for these sources. For both these objects the number of flux density measurements was too small to derive a reliable mean value for 1.4/1.7 GHz. Presently only flux densities at 430 MHz are given in the literature (Nice, Taylor, & Fruchter 1993; Nice & Taylor 1995).

In order to compare the spectra for Galactic disk MSPs and normal pulsars, we used a set of spectral indices for 346 normal pulsars which was derived from data presented by Malofeev et al. (1994), Lorimer et al. (1995b) and also Taylor et al. (1995). We find that the average spectrum of MSPs seems to be steeper than that of normal pulsars, i.e. we derive a mean spectral index of  $-1.8 \pm 0.1$  for a set of 32 MSPs located in the Galactic disk and a mean index of  $-1.60 \pm 0.04$  for normal pulsars in the same frequency range.<sup>6</sup> The median values for both samples are  $-1.8$  and  $-1.7$ , respectively. Although the mean spectrum for MSPs seems to be somewhat steeper, both distributions appear very similar. A Kolmogorov-Smirnov (KS) test yields a probability of 36% that they are drawn from the same parent distribution.

However, as already discussed, the sample of normal pulsars is obviously biased towards distant, flat spectrum sources. Removing this bias by restricting the compared data sets to those sources which are closer than 1.5 kpc, we actually find mean spectral indices which are essentially the same, i.e.  $-1.6 \pm 0.2$  (MSPs) and  $-1.7 \pm 0.1$  (normal pulsars) with median values of  $-1.65$  and  $-1.66$ , respectively. Comparing these distributions of 18 MSPs and 55 normal pulsars (Fig. 1), we find an even higher KS-probability of 50% that the underlying parent distribution is the same. As a final confirmation, we compare the spectral indices of nearby MSPs and normal pulsars detected by the Parkes survey. In this case, we obtain mean spectral indices of  $-1.8 \pm 0.2$  (MSPs) and  $-1.7 \pm 0.1$  (normal pulsars) and a KS-probability of 53% that both distributions are the same. We thus conclude that there is no apparent difference in the spectra of normal pulsars and MSPs. This is somewhat contrary to the first spectral study of 4 MSPs (Foster et al. 1991) in which MSP spectra

---

<sup>6</sup>Errors quoted here correspond to the mean standard deviation of the mean.

appeared to be steeper on average than normal pulsars. The larger sample of objects available to us shows that steep spectra MSPs are the exception rather than the rule.

Obtaining more data at high and low frequencies in the future, i.e., above 2 GHz and below 400 MHz, will provide interesting information, particularly if MSP spectra also show the typical steepening at a few GHz and a low frequency turn-over, which are both often observed for normal pulsars (Malofeev et al. 1994). Indeed, the spectrum of B1937+21 presented by Foster et al. (1991) indicates a low-frequency turn-over.

### 3.2. Luminosities of MSPs

For birth-rate studies of MSPs it is particularly important to compare their luminosities to those of normal pulsars. Since we can estimate the uncertainties of our homogeneous sample of flux densities obtained at 1.4/1.7 GHz better than those of values published for 400 MHz by various authors, we compare distance-corrected flux densities observed at 1.4 GHz for both MSPs and normal pulsars. This is possible since we have seen that the spectra of MSPs and normal pulsars are essentially the same. Consequently, we calculate values  $S \times d^2$ , i.e. flux density measured in mJy (Table 1) times square of the distance in kpc<sup>2</sup>. We find that MSPs are apparently one order of magnitude less luminous than normal pulsars (see Fig. 2). The mean value of  $\log(S \times d^2 [\text{mJy kpc}^2])$  is only  $0.5 \pm 0.2$  for our sample of 31 MSPs located in the Galactic disk<sup>7</sup> compared to  $1.50 \pm 0.04$  for 369 normal pulsars (Lorimer et al. 1995b; Taylor et al. 1995). This is the reason why MSPs appear as relatively weak sources at high radio frequencies, so that only a small number of them could be detected at frequencies as high as 4.85 GHz (Kijak et al. 1997a). Removing the obvious bias from both samples by restricting our analysis to all those sources which are closer than 1.5 kpc, we note that this difference in luminosity becomes less prominent (Fig. 3). We now find mean values for  $\log(S \times d^2)$  of  $0.0 \pm 0.1$  (18 MSPs) and  $0.57 \pm 0.09$  (55 normal pulsars). The corresponding medians are 0.1 (MSP) and 0.5 (normal), respectively. Performing a Kolmogorov-Smirnov test on both samples, we find that both distributions are similar with a probability of 13%. It is interesting that besides a deviating mean value for the luminosity there seems to be a lack of highly luminous sources, i.e.  $\log(S \times d^2) > 1$ , found for MSPs relative to normal pulsars. This could be an artifact due to the smaller number of MSPs in our sample or perhaps due to a possible remaining small difference in the spectral distribution of both samples. However, relying completely on published flux densities we find a similar trend in the (usually) quoted 400-MHz luminosities. It therefore seems that, although normal pulsars and MSPs have fairly similar luminosity distributions, MSPs tend to be slightly weaker sources on the average. In order to verify this result we have performed the same analysis on nearby sources detected in the Parkes survey. The derived values are  $-0.3 \pm 0.3$  and  $0.5 \pm 0.1$  for the mean logarithm of  $S \times d^2$  of MSPs and normal pulsars, while we find medians

---

<sup>7</sup>We did not include PSR J0218+4232 because for this object the distance information is very uncertain (Navarro et al. 1995).

of 0.1 (MSP) and 0.6 (normal), respectively. A KS-probability of only 4.8% is found that both distributions are drawn from the same parent distribution. Summarising, we have indications that the luminosity distributions of both types of pulsars are slightly different.

### 3.3. Relationships to other parameters

Any difference in the emission properties of MSPs and normal pulsars could have its origin in the assumed special evolutionary history of MSPs or the significant difference in period and magnetic field (see also paper II).

It is therefore interesting that although we have only seven (out of nine) isolated MSPs (including the planetary system B1257+12) in our flux density sample, we can confirm the observation by Bailes et al. (1997), that isolated MSPs tend to exhibit lower luminosities than binary MSPs. The mean value of  $\log(S \times d^2)$  for isolated MSPs is only  $-0.1 \pm 0.4$  and thus lower than that for the rest of the sample,  $0.6 \pm 0.1$ . Restricting the sample to those sources within a distance of 1.5 kpc, we still find a difference in the mean value for isolated MSPs ( $-0.5 \pm 0.3$ ) and binary MSPs ( $0.2 \pm 0.1$ ). In contrast, the mean spectral index for isolated MSPs appears to be the same as that for the whole sample,  $-1.7 \pm 0.1$ .

Investigating possible relationships of the spectral properties of MSPs to spin parameters like period, magnetic field, spin down luminosity ( $\propto \dot{P}P^{-3}$ ) or accelerating potential ( $\propto B/P^2$ , e.g., Ruderman & Sutherland 1975), we could not find significant correlations. Calculating these values we have used intrinsic period derivatives, i.e., observed values of  $\dot{P}$  were corrected for kinematic effects whose importance for pulsars was first pointed out by Shklovskii (1970). As a result, measured spin-down rates can be biased by proper motion and Galactic acceleration (see Damour & Taylor 1991), which can become a significant effect for MSPs (Camilo, Thorsett, & Kulkarni 1994). For those sources where no velocity information was available, after Camilo et al. (1994) we assumed a transverse speed of 75 km/s. We note in passing, that there might be a tendency for the spectral index of MSPs to correlate with the characteristic age of MSPs, i.e., younger MSPs tend to have a steeper spectrum than older MSPs. We find that Galactic disk MSPs with a characteristic age between  $10^8$  yr and  $10^9$  yr have a mean spectral index of  $-2.5 \pm 0.3$ , while those with a characteristic age between  $10^9$  yr and  $10^{10}$  yr exhibit a mean spectral index  $-1.9 \pm 0.2$ . MSPs with a characteristic age larger than  $10^{10}$  yr in comparison show a mean index of  $-1.4 \pm 0.2$ . This trend would be in apparent contrast to that observed for normal pulsars (Johnston et al. 1992; Lorimer et al. 1995b). As new sources are discovered, it will be interesting to see whether this tendency still holds. However, the lack of any significant correlation between spectral properties and observed spin parameters is similar to the observations made for normal pulsars assuming a canonical pulsar model (Malofeev 1996).

Investigating the radio efficiency of MSPs and normal pulsars we have compared the ratio of spin down luminosity,  $\dot{E} = 3.95 \cdot 10^{46} \dot{P}P^{-3}$  erg/s where  $P$  is measured in seconds (e.g., Manchester



& Taylor 1977), and observed radio luminosity. The distribution of the logarithm of this ratio,  $S \times d^2/\dot{E}$ , expressed in units of  $\text{mJy kpc}^2 \text{erg}^{-1} \text{s}$  is presented in Fig. 4 for both MSPs and normal pulsars. Again we have restricted both samples to sources closer than 1.5 kpc to remove the bias previously discussed. It is evident that MSPs are much less efficient radio pulsars than slow rotating ones. The mean value of  $\log(S \times d^2/\dot{E})$  found for MSPs and normal pulsars is  $-33.3 \pm 0.2$  and  $-31.5 \pm 0.1$ , respectively, while the mean value of  $\log \dot{E}$  itself is found to be  $33.2 \pm 0.1$  (MSP) and  $32.0 \pm 0.1$  (normal), respectively.

#### 4. Pulse shapes of millisecond pulsars

In Figs. 10–13 we present a collection of 27 profiles of MSPs.<sup>8</sup> They all represent averages of typically ten to twenty independent observations and were used as templates for timing purposes. Most of the profiles are of unprecedented quality in signal-to-noise ratio and resolution. Both are indicated by the small error box left of the pulse. The height of the box corresponds to one standard deviation (RMS) measured in an off-pulse region while its width represents the resolution of the profile. The latter is determined by the dispersion smearing across one filterbank channel of 666 kHz. Only for B1744–24A and B1937+21 is this dispersion smearing apparently large enough to smear out individual features of the pulse shape, also having a significant impact on the measured width of the profile presented in Table 2. For B1937+21 we therefore present a pulse profile which was obtained with the EBPP, a coherent dispersion removal processor recently installed in Effelsberg. Details of this system are published elsewhere (Backer et al. 1997). For the other profiles presented the indicated effective resolution of the profile, also quoted in Table 2, is that imposed by interstellar dispersion, since we sampled each profile with a resolution of  $P/1024$  s which is generally smaller than the smearing time. In the few cases, where sampling time and dispersion smearing become comparable, the effective resolution is the sum in quadrature of both.

##### 4.1. Newly detected morphological features

A detailed discussion of individual pulse profiles is presented in paper II using their polarisation properties to gain further insight in the nature of the various components. In this paper we want to draw attention to a few particular sources where the quality of the profiles obtained is so good, that previously undetected profile features have been discovered or where previously known features are significantly better resolved in our observations.

As a first example we note J1518+4904 whose pulse is relatively narrow compared to the majority of MSPs. It exhibits a significant post-cursor (see arrow in Fig. 10). This post-cursor

---

<sup>8</sup>These data are freely available in the European Pulsar Network Data Archive: <http://www.mpifr-bonn.mpg.de/pulsar/data/>

follows the midpoint of the main profile after about  $25^\circ$  and seems to be connected to it by low intensity emission. Details can be better seen in Fig. 14 where we plot the bottom of the profile magnified.

Another post-cursor is detected for J1730–2304, which is separated from the midpoint of the profile by about  $120^\circ$  (cf. arrow in Fig. 11). We could not detect any emission connecting main pulse and post-cursor (see Fig. 14).

Another interesting case is J1744–1134 which exhibits a pre-cursor preceding the main pulse by about  $124^\circ$  (or following the main pulse by about  $236^\circ$  as in Fig. 11). Inspecting the magnified profile in Fig. 14 we also note the possible existence of a feature following the profile by about  $80^\circ$ . Further observations are required to establish the existence of this post-cursor.

While the existence of the pre-cursors of J2145–0750 is well known (Lorimer 1994), we can confirm the pre-cursor of B1953+29 first observed by Thorsett & Stinebring (1990, cf. Fig. 12). We finally draw the attention to J2317+1439. For this pulsar we detect a prominent post-cursor, following the midpoint of the profile by about  $70^\circ$  but connected to the main profile by low level emission. Additionally, we note the possible existence of a weak interpulse preceding the main pulse by about  $150^\circ$ .

## 4.2. Complexity of pulse profiles

The complicated profiles of some of the first discovered MSPs (e.g., B1953+29, B1957+20) created the impression that MSP profiles are much more complex than those of normal pulsars which would be tempting to relate to the evolution history of MSPs by a possible disturbance of the magnetic field structure due to mass accretion (Ruderman 1991). As now about 40 MSPs are known in the Galactic plane, it seems adequate to re-examine this issue again in the light of a much larger sample presented here.

A measure of the complexity of pulse profiles is obviously given by the number of Gaussian components needed to obtain a representation of the pulse profile. Using a method described by Kramer et al. (1994), which assures that random noise features are not misinterpreted as spurious pulse components, we follow Foster et al. (1991) and have separated the pulse shapes into individual Gaussian components. For each profile, the components obtained are indicated by the dashed lines in Fig. 10–13. In order to compare them to a large sample of normal pulsars, we applied the same component separation method to 180 profiles of normal pulsars presented by Seiradakis et al. (1995). Since all profiles were observed at the same frequency using the identical observing system EPOS and by applying the same time resolution, both samples are ideal for a comparison of the profiles of normal pulsars and MSPs. Additionally, due to the very interesting shape of PSR J0437–4715, we included the 1520 MHz profile presented by Bell et al. (1997) in our analysis which is comparable in quality and resolution to the Effelsberg data.

Separating MSP profiles into components we find that they exhibit on average  $4.2 \pm 0.4$  Gaussian components. For normal pulsars we derive a mean number of components, which is smaller by one unit,  $3.0 \pm 0.1$ . The sample of normal pulsars contains a large number of profiles with more than five components. This is mostly due to the existence of multi-component interpulses (e.g., B1929+10) but also due to such complex profiles as B0740–28 (cf. Kramer 1996) or B1237+25, B1742–30 and B1952+29 (Seiradakis et al. 1995). On the other hand, the sample of MSPs contains the very complex profiles of J0437–4715 (12 components) and J1012+5307 (9 components). Comparing the medians of the number of components, we however, find the same result, i.e., a median of 4 for MSPs compared to 3 for normal pulsars. Fig. 5 shows the distribution of both samples, demonstrating that the majority of MSP profiles can be described by only three to four components.

It is important to note that in the analysis described we included components representing interpulses or post- and pre-cursors. While only about 2% of all normal pulsars are known to exhibit interpulses or pre/post-cursors (Lyne & Manchester 1988; Seiradakis et al. 1995; Taylor et al. 1995), about 36% of all Galactic MSPs known either emit a post- or pre-cursor, or exhibit an interpulse. This apparent characteristic of MSPs has been noted before in particular for the occurrence of interpulses, albeit in a much smaller sample (Ruderman 1991). This is an important distinction between these two classes of objects, which also accounts for some of the difference in the complexity. In summary, we conclude that the difference in the complexity of pulse shapes of MSPs and normal pulsars is surprisingly small (i.e., only one Gaussian component). Simultaneously, we consider the peculiar large number of MSP interpulses and pre/post-cursor as an important clue in deciphering the circumstances in their very compact magnetospheres (cf. paper II).

### 4.3. Shape of the emission beams

If the emission beam of radio pulsars is confined to the open field line region, simple scaling arguments based on the opening angle of the last open field lines (Goldreich & Julian 1969) suggest that the radiation beam of MSPs should be larger than that of normal pulsars. As a first approximation for the size of the beam one can study the observed profile widths which are listed in Table 2 for our sample of MSPs. These widths were obtained using the technique described by Kramer et al. (1994) and are quoted for a 50% and 10% intensity level, which refer to the peak of the outermost resolved components. Quoted 10%- and 50%-widths,  $W_{10}$  and  $W_{50}$ , represent only the value measured for the main pulse, i.e., possible interpulses are not included. Post- and pre-cursors are only considered in the calculations if their intensity exceeds the 10% intensity level. Additionally, we present the equivalent pulse width,  $W_{\text{eq}}$ , defined as the width of a box-car like pulse shape of the same energy and amplitude as measured for the real pulse. Generally, a large ratio of  $W_{50}/W_{\text{eq}}$  indicates the presence of prominent outer components. All widths and their corresponding uncertainty, which is mainly determined by the dispersion smearing, are quoted in both units of degrees of longitude and milliseconds. Additionally, we used the value of  $W_{10}$  to derive the duty cycle of the pulsed emission.

MSP profiles typically have a considerably larger duty cycle than normal pulsars, as indicated by Fig. 6, where we have plotted  $W_{10}$  as a function of pulse period. Values of  $W_{10}$  for normal pulsars were taken from Gil, Kijak, & Seiradakis (1993) and Kramer et al. (1994) who used the same observing system and frequency as used to obtain the data presented here. Although the effects of dispersion and sampling generally increase the width of the MSPs more than the normal pulsars, the *relative* resolution of our MSP data (i.e. 4.2% of the period in the worst case of B1744–24A compared to more typical values of less than 1%) is very similar to that of normal pulsars, so that the generally larger duty cycle is clearly significant. However, the pulse width is only a poor estimator for the true size of the emission beam since it is significantly biased by the individual viewing geometry of each pulsar.

The observed pulse width depends strongly on the inclination angle  $\alpha$  between the rotation and magnetic axis and the impact parameter  $\beta$ , which describes the closest (angular) approach of our line-of-sight to the magnetic axis. Usually,  $\beta$  is defined to be positive if line-of-sight and rotation axis are located on opposite sides of the magnetic pole (cf. Lyne & Manchester 1988). In this framework, the actual angular *radius* of the emission beam,  $\rho$ , and an observed pulsed width,  $W$ , are related by

$$\sin^2\left(\frac{W}{4}\right) = \frac{\sin^2\left(\frac{\rho}{2}\right) - \sin^2\left(\frac{\beta}{2}\right)}{\sin\alpha \cdot \sin(\alpha + \beta)} \quad (1)$$

(e.g., Gil, Gronkowski, & Rudnicki 1984). Knowing the emission geometry, one can use  $\alpha$ ,  $\beta$  and an observed width  $W_{10}$  to derive the opening angle of the beam at a 10%-level,  $\rho_{10}$ , which corresponds to the angular radius of a circular radiation beam.

In the ideal case,  $\alpha$  and  $\beta$  can be derived from polarisation data by fitting the classical rotating vector model (Radhakrishnan & Cooke 1969) to the observed swing of the position angle (e.g., Blaskiewicz, Cordes, & Wasserman 1991; Hoensbroech & Xilouris 1997a). For normal pulsars the viewing geometry has been determined for a large sample (e.g., Lyne & Manchester 1988; Blaskiewicz et al. 1991; Rankin 1993a,b), so that  $\rho_{10}$  could be determined. In Fig. 7 we plot opening angles for normal pulsars derived from profiles observed at a frequency of 1.4 GHz which were again taken from data presented by Gil et al. (1993) and Kramer et al. (1994). Since the profile width is generally a function of frequency, we could not include the large sample presented by Rankin (1993b), since these data were scaled to a lower frequency of 1 GHz. The large scatter visible in the width-period plot of normal pulsars (Fig. 6) disappears and the opening angle of normal pulsars seems to follow a  $P^{-0.5}$ -dependence which had been pointed out by Rankin (1993a) and later confirmed by Gil et al. (1993), Gould (1994) and Kramer et al. (1994; see also Biggs 1990). This period dependence is the same as that for the opening angle  $\rho_0$  of the last open field line in a dipolar field structure. For a given emission height  $R_{\text{em}}$  one obtains the relationship:

$$\rho_0 = \sqrt{\frac{9\pi R_{\text{em}}}{2Pc}}, \quad (2)$$

where  $\rho_0$  is measured in radians,  $c$  is the speed of light ( $\text{m s}^{-1}$ ), and  $P$  is the pulse period (s).

While the  $P^{-0.5}$ -dependence of the opening angle has been independently determined, the details of the scaling law (e.g., the actual scaling factor or a possible bi-modality of the distribution) differ slightly among the various authors. In any case, the relation obtained and the maximum possible value for  $\rho$  of  $90^\circ$ , corresponding to a duty cycle of unity and thus continuous emission, limit the period to a minimum value possible theoretically for pulsed emission. In other words, if the scaling law derived for normal pulsars applies also to MSPs, a detection of MSPs with periods below this critical period might not be possible. For a frequency of 1.4 GHz, Gould (1994) derives a lower bound for the opening angles given by  $\rho_5 = 5.4^\circ \cdot P^{-0.5}$  measured at a 5%-intensity level, while Gil et al. (1993) present  $\rho_{10} = (4.9^\circ \pm 0.5^\circ) \cdot P^{-0.48 \pm 0.03}$  and Kramer et al. (1994)  $\rho_{10} = (5.3^\circ \pm 0.3^\circ) \cdot P^{-0.45 \pm 0.04}$  for a lower bound valid at a 10%-intensity level. These scaling laws would imply a minimum possible period between 1 ms and 4 ms, which would be just consistent with the shortest periods actually observed. Moreover it would suggest that, if the neutron star equation-of-state allows the existence of sub-millisecond pulsars, such objects might exhibit substantially different emission properties. Obviously, it is very interesting to see whether the scaling laws obviously present for normal pulsars are also valid for MSPs. In the following we therefore attempt to derive the opening angle of the beam for a number of MSPs.

The polarisation data of MSPs presented in paper II are used to model the observed position angle swing in order to obtain information about the viewing geometry and the emission heights (paper III). For fourteen sources, fits assuming the classical rotating-vector-model are made and  $\alpha$  and  $\beta$  determined. Corresponding values derived for the opening angle are presented in Table 3 and plotted in Fig. 7 as a function of period. The viewing geometry for B1534+12 presented by Arzoumanian et al. (1996) and that presented for B1855+09 by Segelstein et al. (1986) are consistent with the results of paper III by yielding the same opening angles within the uncertainties. For PSR B1913+16, Cordes, Wasserman, & Blaskiewicz (1990) find constraints for the angles  $\alpha$  and  $\beta$ , from which we can derive  $\rho_{10} = 21 \pm 4^\circ$ .

Although fitting the position angle swing is certainly the best way to obtain estimates of the individual  $\alpha$  and  $\beta$  values (cf. Lyne & Manchester 1988; Rankin 1990), the results might be sometimes only poorly constrained (e.g., Hoensbroech & Xilouris 1997a). In fact, the uncertainties of  $\rho_{10}$  presented in Table 3 and Fig. 7 for both normal pulsars and MSPs reflect only the estimated error in the used pulse width. However, very often the derived opening angles agree within these uncertainties if values for  $\alpha$  and  $\beta$  are used which were derived independently by various authors (see, e.g., Kramer et al. 1994). Nevertheless, we tried to find a second way to get an estimate for the opening angle which is *independent* of derived values for  $\alpha$  and  $\beta$ . We developed a new method to constrain the actual value of  $\rho$  statistically. This is described in the following.

For an observed width of the pulse profile, a certain combination of  $\alpha$  and  $\beta$  (or  $\alpha$  and  $\sigma \equiv \alpha + \beta$  as used hereafter) leads to a value of  $\rho$  fulfilling Eq. (1). The angles  $\alpha$  and  $\sigma$  are both defined in the interval  $[0; \pi]$ . One can thus test how often a certain value for  $\rho$  could explain the observed width for the given parameter space. While we cannot make any *ad hoc* assumption about the distribution of  $\alpha$ ,  $\sigma$  as a purely geometrical factor of the relative orientation of pulsar and Earth, should be

distributed uniformly, so that the observed distribution is derived by weighting the possible  $\rho$  values by a factor  $\sin\sigma$ . For a given profile width we find typical probability distributions  $p(\rho)$  as presented in Fig. 8. The most likely value for the opening angle is given by the peak of the distribution function. In the following, we however use the typically larger expectation value  $\langle\rho\rangle$  given by  $\langle\rho\rangle = \int p(\rho') \rho' d\rho'$ . We can also derive an upper limit of  $\rho$  which is valid with a certain probability. For a probability of 68%, such upper limit  $\rho_{\max}$  is given by  $\int_0^{\rho_{\max}} p(\rho') d\rho' = 0.68$ . Both values are presented for a number of MSPs in Table 3 and Fig. 7. The expectation value  $\langle\rho\rangle$  is plotted as a triangle while its error bar indicates the upper limit  $\rho_{\max}$ , i.e. with a probability of 68% the actual value of  $\rho$  is smaller than the one indicated. We stress that these statistical estimates do not depend on the determination of  $\alpha$  and  $\beta$ .

In Fig. 7 we compare the opening angles of normal pulsars and MSPs. We have plotted the lower bound  $\rho = 5.4 \cdot P^{-0.5}$  derived by Gould (1994, dashed line). Additionally, we indicate the maximum possible value of  $\rho$  of  $90^\circ$  by a dotted line. Assuming dipolar magnetic field lines (Eq. 2), we have marked the region of opening angles which corresponds to the interior of a neutron star of 10 km radius. With the same assumption one can use Eq. (2) to translate the opening angle into an emission height in units of fraction of the light cylinder radius,  $R_{LC} = c P/2\pi$ . A corresponding scale is indicated on the right hand side of the plot.

It is obvious from our sample of 27 MSPs that three sources have statistical values larger than predicted by the scaling law derived from the sample of normal pulsars (J0621+1002, B1802–07 and J2145–0750), while only five MSPs (i.e. B1620–26, J1730–2304, B1744–24A, B1913+16 and B1953+29) exhibit opening angles which are consistent with this scaling law. In fact, the large majority of opening angles derived for MSPs are significantly smaller than expected (note the logarithmic scale). A similar statement has been already made for the pulse width of B1937+21 by Chen & Ruderman (1993; see also Backer 1995) although we have demonstrated that the pulse width itself is only a poor estimator to learn more about the size of the emission beam. Here we have derived opening angles and thus attempted to remove geometrical effects which are always present. For three sources (J1640+2224, J1744–1134 and J2317+1439) the derived values are not only smaller than expected but they even indicate that the emission takes place *inside* the neutron star. For the other sources, the indicated emission heights are substantially closer to the neutron star than those derived for normal pulsars. However, due to the compactness of MSP magnetospheres, the emission height is nevertheless at a significant fraction of the light cylinder radius, i.e. at 10% to 50% compared to the at most few percent observed for normal pulsars (e.g., Cordes 1978; Matese & Whitmire 1980; Cordes & Stinebring 1984; Blaskiewicz et al. 1991; Phillips 1992; Xilouris et al. 1996).

#### 4.4. Frequency development of pulse profiles

Normal pulsar profiles very often show a distinct profile development with frequency which can be used for a classification scheme, such as the one devised by Rankin (1983). Comparing the

frequency development of pulse profiles of normal pulsars and MSPs between 400 MHz and 1400 MHz, one gets the impression that MSP profiles change much less with frequency than normal pulsars. A detailed discussion of individual MSP profiles and their frequency development is given in paper II. Here we just want to investigate whether this tendency is related to the assumed evolutionary history of MSPs. In such a case, the profiles could be affected by the amount of mass transferred from the binary companion since the transferred mass could have altered the dipolar magnetic field structure of the progenitor and thus the profile development compared to normal pulsars (Ruderman 1991).

In order to quantify the profile development of MSPs we have used the results of the component separations (see Sect. 4.2) to produce noise-free templates. These templates were modified by adjusting the individual components to match the profiles observed at lower frequencies (in cases where low-frequency data were available in digital form, these data were used; for references see Table 1). The normalised difference in the area defined by the two pulse shapes,  $\kappa$ , was finally used as the parameter describing the profile change, i.e.

$$\kappa = \sum_{i=1}^n \left| \frac{t_i(\nu_1)}{\sum_{j=1}^n t_j(\nu_1)} - \frac{t_i(\nu_2)}{\sum_{j=1}^n t_j(\nu_2)} \right|. \quad (3)$$

The noise-free templates obtained for frequencies  $\nu_1$  and  $\nu_2$ , are represented by  $n$  samples,  $t_1, \dots, t_n$ . While  $\nu_1$  was 1.41 GHz,  $\nu_2$  was generally taken to be 400 MHz (Table 1). A value close to unity means a large development in frequency while a value close to zero means a small change in the profiles. The parameter,  $\kappa$ , could be determined for those profiles of MSPs in the Galactic disk for which profiles of considerably good resolution and quality at low and high frequencies were available. Profiles of B1937+21 were excluded since they are affected by interstellar scattering at low frequencies (Thorsett & Stinebring 1990).

Since high-mass binary pulsars are expected to have accreted a smaller amount of mass than low-mass binary pulsars with large inferred amounts of accreted mass (e.g., Phinney & Kulkarni 1994), we plotted  $\kappa$  versus the companion mass (Fig. 9). In cases where the inclination of the binary system is not known, we assumed the most probable angle of  $60^\circ$  to calculate the mass of the companion. We observe a slight tendency for systems with less massive companions to show more profile development with frequency than those with more massive companions. The mean value of  $\kappa$  for systems with companion masses  $m_c \leq 0.45M_\odot$  is  $0.37 \pm 0.05$  (12 sources) but only  $0.22 \pm 0.05$  for those with  $m_c > 0.45M_\odot$  (6 sources, Fig. 9).

It can be expected that the final spin period of a recycled pulsar is related to the companion mass (e.g., van den Heuvel & Bitzaraki 1995). Studying  $\kappa$  as a function of pulse period we see, in fact, essentially the same tendency. Distinguishing between sources with spin periods smaller and larger than 10 ms (now also including isolated MSPs with reasonably resolved profiles), we find a mean  $\kappa$  of  $0.35 \pm 0.05$  for  $P \leq 10$  ms (16 sources) and  $0.21 \pm 0.03$  for  $P > 10$  ms (8 sources). It will be interesting to see whether this apparent tendency remains valid as more MSPs in massive binary systems and with larger spin periods are discovered.

## 5. Discussion

In Sect. 3 we have demonstrated that MSPs and normal pulsars exhibit the same flux density spectrum. While MSPs appear to be less luminous compared to normal pulsars, we have also seen that MSPs are less efficient radio sources. In particular, we confirm the observation by Bailes et al. (1997), that binary MSPs are more luminous than isolated MSPs, while we show simultaneously that both groups exhibit the same mean spectral index. Although we observe a weak tendency that the characteristic age is correlated with the spectral index of MSPs, no other significant correlation between spectral properties of MSPs and other system characteristics is apparent.

Investigating the complexity of pulse profiles of normal pulsars and MSPs, we have demonstrated that, on average, MSP profiles are only marginally more complex than those of normal pulsars. In fact, the intrinsic size of MSP radiation beams is much smaller than expected from the scaling laws derived for normal pulsars. We observe the tendency that the profile development with frequency is related to the amount of mass transferred during the recycling process.

### 5.1. MSPs as radio sources

The sample of sources presented in Table 1 misses only two Galactic MSPs within a distance of 1.5 kpc, which have no published detection at 1400 MHz (J0034–0534 and J1455–3330). These non-detections suggest a steep spectrum for both sources which could lead to a slightly steeper mean spectral index for all MSPs. The same however applies also to our sample of normal pulsars where we also included only those sources which were previously detected at 1400 MHz. We therefore conclude that the comparison of both samples leads to reliable results. We note in passing that the mean spectral index of those four sources detected by Kijak et al. (1997a) at 4.85 GHz is  $-1.53 \pm 0.09$  and thus smaller than the mean spectral index for the whole sample, as expected.

The result that the spectra of normal pulsars and MSPs are essentially the same, strongly suggests the same emission mechanism for both types of pulsars, in spite of the difference in period by three orders of magnitude. If the magnetic field structure in the emission region is influencing the flux density spectrum, as in the case for curvature radiation, this result points also towards a dipolar field structure as found for normal pulsars. In such a case, the emission mechanism must also work over four orders of magnitude in magnetic field strength as inferred by the measured period derivatives. However, multipole components existing at the neutron star surface could increase the magnetic field strength over the value expected from a dipolar field structure (see Krolik 1991; Arons 1993; paper II). In any case, the weak tendency of a correlation between the spectral index and the characteristic age, which is in contrast to that observed for normal pulsars, suggests an evolution of the magnetospheric conditions.

Our observations show that MSPs tend to be less luminous than normal pulsars, while they are also less efficient radio emitters compared to normal pulsars. During the analysis leading to this



result we used a luminosity estimator defined as the observed equivalent continuum flux density, i.e., measured pulse energy,  $E_R$ , averaged over the pulse period,  $S = E_R/P$ , times the square of the distance (cf. Manchester & Taylor 1977). Most of the distances used for both normal pulsars and MSPs are derived from dispersion measures using the model by Taylor & Cordes (1993). The resulting values are therefore somewhat uncertain. However, our conclusions are based on samples of objects within 1.5 kpc distance, where the Taylor & Cordes (1993) model should be free of systematic trends. Any remaining effect not accounted for in this model, would apply to both groups of objects, and thus would not change our result. Actually, a more severe effect to be considered is the disadvantage of the luminosity estimator in that it reflects only the emission received by the cut of our line-of-sight rather than that from the full emission cone. The derived luminosity is thus also biased by the viewing geometry. In order to account for this effect one should make use of derived opening angles to use the true size of the emission beam in order to calculate the luminosity. For a comparison of sources we had to assume filled emission beams of circular shape. Moreover, the opening angles can only be determined for a limited number of sources, so that we decided to use a second luminosity estimator based on the peak flux density,  $S_{\text{peak}}$ , which still depends on the viewing geometry but is less affected by the actual pulse shape and width. The previously used luminosity is defined as  $S(\text{mJy}) \times d^2(\text{kpc}^2) = E_R(\text{mJy s}) \times d^2(\text{kpc}^2) / P(\text{s})$ , which using the definition of the equivalent width becomes  $S(\text{mJy}) \times d^2(\text{kpc}^2) = S_{\text{peak}}(\text{mJy}) \times W_{\text{eq}}(^{\circ}) \times d^2(\text{kpc}^2) / 360^{\circ}$ . We have thus computed the value  $L_{\text{peak}} \equiv 360^{\circ} S(\text{mJy}) \times d^2(\text{kpc}^2) / W_{\text{eq}}(^{\circ})$  using the equivalent widths presented in Table 1 and those published by Gould (1994) for normal pulsars. For normal pulsars within a distance of 1.5 kpc we find a mean value for  $\log L_{\text{peak}}$  at 1400 MHz of  $2.11 \pm 0.09$  with a median of 2.07. In contrast, for our sample of MSPs closer than 1.5 kpc we find a mean value for  $\log L_{\text{peak}}$  of  $1.4 \pm 0.2$  with a median of 1.5. The KS-probability that both distributions are drawn from the same parent distribution is only 1%, strengthening even further the conclusion that MSPs are less luminous than normal pulsars.

It is interesting to note that MSPs seem also to be less efficient gamma-ray sources since from the six pulsars confirmed as EGRET sources, none is a MSP (Kanbach et al. 1996). This fact is surprising since the mean value of  $\dot{E}$  for MSPs is more than one order of magnitude larger than that of normal pulsars (cf. Sect. 3.3). Moreover, most of the known MSPs are nearby sources due to the afore-mentioned selection effects, so that the ratio of  $\dot{E}$  and square of the distance,  $\dot{E}/d^2$ , apparently relevant for gamma-ray emission, is much larger for MSPs than for the average normal pulsar. One can speculate whether these observations for radio and gamma-ray emission are related since for both types of radiation, similar models are proposed, i.e., polar cap and outer gaps models (cf. paper II). While the sample of slowly-rotating pulsars detected as gamma-ray sources is made up by relatively energetic pulsars, a difference in the particle density in the magnetosphere of normal pulsars and MSPs could explain the dissimilarity in their luminosity distribution. The fact that there is a difference in the radio luminosity distribution of binary and isolated MSPs strongly suggests that the luminosity of all MSPs is affected by their evolutionary history.

## 5.2. The beam structure of MSPs

It has been suggested that the overall dipolar field apparently observed for normal pulsars (e.g., Phillips & Wolszczan 1992; Kramer et al. 1997) could be distorted by the existence of magnetic multipoles in cases of MSPs which could be enhanced by mass accretion from a binary companion. Disturbance of a dipolar field structure or the existence of magnetic multipoles in the emission region should be reflected by overall shape of pulse profiles, their frequency development, and in particular in the polarisation properties which are discussed in detail in paper II.

### 5.2.1. Complexity of pulse profiles

The previously observed apparent large complexity of MSP profiles was attributed to a deviation of the magnetic field structure from a dipolar form (Krolik 1991). However, we have demonstrated that the majority of MSP profiles are actually only marginally more complex. Since most of the profiles used to derive this result are in general of very high resolution already, we do not expect the observable complexity to change significantly even if a coherent de-dispersion technique is used (cf. profile of B1937+21 and also Backer 1995).

We believe that the impression created after the discovery of only a few MSPs, was mainly due to the much larger duty cycle seen (see Table 2). In contrast to the average 3% found for normal pulsars (Taylor et al. 1995), we observe a mean duty cycle of 21% for MSPs. Therefore, for MSPs one immediately observes a “blown-up” version of the pulse shape, enabling an easier identification of various components. Zooming in on the profiles of normal pulsars as done by Seiradakis et al. (1995) or Kijak et al. (1997b), can lead to similar results for normal pulsars. Therefore, the complexity of MSP profiles alone does not obviously provide any clue as to whether higher order magnetic multipoles exist in the emission region. In fact, if the number of components is related to the size of the polar cap, one would expect a considerably larger number of components for MSPs even in cases of a dipolar field, since the polar cap scales as  $P^{-0.5}$ . This is however not the case. As already discussed, a perplexing large number of interpulses and pre-/post-cursors makes up for some of the one unit difference derived in the mean number of components of normal pulsars and MSPs. Therefore, even if a dipolar field near the neutron star or in the emission region exists, the full open field line region might not be illuminated. In any case, the large number of additional pulse features appearing in addition to the main pulse is an important significant difference in the properties of MSP and normal pulsar emission. Combined with the relatively normal complexity of MSP profiles, it possibly suggests that their origin is due to additional radiation beams, e.g., due to outer gap emission (e.g., Cheng et al. 1986). We discuss this possibility further in paper II.

### 5.2.2. Beam size

By investigating the opening angles, we have demonstrated that the radiation beams of MSPs are significantly smaller than expected. Certainly, the opening angles based on a determination of the viewing geometry by studying polarisation data (paper III), involves the assumption of the validity of the rotating vector model for MSP magnetospheres to derive  $\alpha$  and  $\beta$ . However, we have seen that the statistically derived opening angles imply the same result. The calculation of  $\rho$  itself does not include any assumption about the magnetic field configuration. It is even independent of the actual shape of the beam, i.e., whether it might be circular or elongated in either latitudinal or longitudinal direction. We suggest three reasons for the different behaviour of MSPs and normal pulsars. The beams might be intrinsically smaller (i.e., the open field line region is not completely filled by emission in contrast to normal pulsars), the emission height or a radius-to-frequency mapping might be different for normal pulsars and MSPs, or the field configuration in MSPs magnetosphere is indeed disturbed as compared to a dipolar field presumably dominant in normal pulsars.

Arons (1993) has used the observed spin-down rates to argue that magnetic multipoles are not prominent in MSP magnetospheres. Again, we focus on this issue in detail in paper II, where for the first time a large homogeneous set of polarisation data is available to trace the magnetic field structure. Here we draw attention to the fact that by assuming dipolar field lines, the derived opening angles lead to inconsistent results, i.e., emission from *inside* the neutron star. This result is however partly based on the assumption of the correctness of the rotating-vector-model fits and a neutron star radius of 10 km. As only a ridiculously small neutron star radius of 1 km can solve this apparent contradiction, the reliability of the polarisation fits is discussed in paper III.

For normal pulsars the observed data suggest that the emission height above the surface is a function of frequency, i.e., high frequency emission is emitted closer to the neutron star than low frequency emission (Cordes 1978). If such a model is also valid for MSPs, then the observed discrepancy between the opening angles of MSPs and normal pulsars could be explained by a different *radius-to-frequency mapping* behaviour, i.e., a different frequency dependence or a change in the absolute scale (cf. Eq. 2). Comparing the  $\rho$ – $P$ -relations derived for normal pulsars at different frequencies (Rankin 1993a,b; Gil et al. 1993; Gould 1994; Kramer et al. 1994), one notes only a very small difference in the scaling factor of the order of one degree of longitude. Given the small frequency development of MSP profiles (cf. Sect. 4.4) it becomes obvious that a different frequency scaling cannot account for the apparent small beam sizes of MSPs. Although the tendency that the profile development is related to spin period or the amount of mass transferred to the MSP is far from being established, its confirmation would in fact suggest that a (probably weak) radius-to-frequency mapping is acting in a non-dipolar field structure. Compared to a purely dipolar field, a small change in the emission altitude should have a larger impact in a disturbed magnetic field structure, causing a larger change in the profile with frequency. Chen & Ruderman (1993) argued that mass accretion would reduce the radius of the polar cap and thus the size of the open field line region. Therefore, the recognised trend in the profile development might not only point towards

the modification of a dipolar field structure by mass accretion, but could also offer an explanation for the smaller beam sizes. In any case, it seems necessary to include additional independent information to decide whether a multipole or disturbed dipolar magnetic field or systematically unfilled emission beams are present. A major step in this direction is taken in papers II and III, where we focus on the possible impact of gravitational bending and magnetic field sweep back. The latter effects are apparently not important for the emission of normal pulsars (e.g., Phillips 1992; Kramer et al. 1997), but they might become relevant if the emission simultaneously takes place close to the neutron star surface and at a significant fraction of the light cylinder radius as indicated by Fig. 7.

### 5.3. Implications for the birth-rate of millisecond pulsars

We have seen that normal pulsars and MSPs apparently differ in the luminosity distribution and the intrinsic size of their emission beam. Both properties are important parameters for deriving the birth-rates of both groups of pulsars.

In general, one will assume as a first approach the same luminosity distributions for MSPs and normal pulsars. However, the observed difference in the mean value of the derived luminosity corresponds to a factor of about six and is therefore at a level to become important for birth-rate studies of MSPs. Indeed, in a recent analysis, Lyne et al. (1998) find evidence for a difference in the luminosity function between normal pulsars and MSPs at low luminosities.

Similarly, one should reconsider the calculated birth-rates of MSPs under the impression that the scaling law for the beam size derived for normal pulsars does not apply to MSPs. Assuming a random distribution of the inclination angle  $\alpha$ , the beaming fraction,  $f$  describing the fraction of the sky covered by the radiation beam, is given by

$$f = (1 - \cos \rho) + \left(\frac{\pi}{2} - \rho\right) \sin \rho \quad (4)$$

(Emmering & Chevalier 1989). If the beaming fraction is large, the chance of detecting a source is high, resulting in a smaller birth-rate necessary to sustain the observed population, compared to the case of a smaller beaming fraction. We have seen that if we apply the scaling law found for normal pulsars also to fast rotating pulsars, the beaming fraction should be very close to unity, i.e.  $f \approx 1$ . In contrast, inspecting Fig. 7, one might get an impression that  $20^\circ < \rho < 50^\circ$  represents a typical value for MSPs, corresponding to a beaming fraction of  $0.5 < f < 0.9$ . An increase in the needed birth-rate can only be avoided if the radiation beam is not circular in shape, but actually elongated in latitudinal direction (cf. Chen & Ruderman 1993). The evidence for elongation of the beam is however weak, and while Narayan & Vivekanand (1983) have indeed suggested such a beam shape, Biggs (1990) even argued for a compression of the beam in the latitudinal direction, depending on the inclination angle.

## 6. Summary

The study of the characteristics of MSP radio emission of which the present work is the first of a series of papers, was motivated by the question, in what respect do MSPs differ from normal pulsars. The fact that both populations exhibit identical flux density spectra points towards the same emission mechanism, which is further supported by the results presented in paper II. At the same time, the radio output of MSPs seems to be affected by their particular evolutionary history, i.e., the entire sample tends to be less luminous and in fact less efficient radio emitters compared to normal pulsars. It is particularly interesting that, compared to the luminosity distribution of normal pulsars within a distance of 1.5 kpc (Fig. 3), we are apparently missing some high luminosity MSPs, although they should be the easiest to detect. Although no significant correlations between spectral parameters and intrinsic spin parameters are observed, we note a weak tendency for old MSPs to exhibit flatter spectra than MSPs with smaller intrinsic ages.

Although remarkable exceptions to the rule are observed, the pulse profiles of MSPs are only slightly more complex than for the normal pulsars. These profiles do not change significantly with frequency (for a detailed discussion see paper II), but we have indications that a measure of profile change is actually related to the amount of mass transferred onto the neutron star during a spin-up episode, or to the spin period. Moreover, the angular beam radii inferred from the observed pulse shapes imply that the emission beam of rapidly-rotating pulsars is smaller than expected from our knowledge of normal pulsars. If the neutron star equation-of-state allows the existence of sub-millisecond pulsars, their detection will thus not be prevented by a beam size being too large as it would have been implied from simply scaling the trend seen in normal pulsars.

The present data suggest that, although MSPs and normal pulsars exhibit the same emission physics, they show pronounced differences probably related to the different evolutionary history. In paper II we elaborate on these aspects further and again raise the question about the origin of these differences in light of the additional data.

We strongly suggest that birth-rate calculations of MSP be reconsidered given the data discussed here.

We are grateful to the operators and engineers in Effelsberg for their support during this project. It is also a pleasure to thank Norbert Wex for extremely helpful discussions leading to the results presented in Sect. 4.3. We thank Alexis v. Hoensbroech, Jarek Kijak and Christoph Lange for their help with the observations. FC gratefully acknowledges the support of the European Commission through a Marie Curie fellowship, under contract no. ERBFMBICT961700. This work was in part supported by the European Commission under the HCM Network Contract Nr. ERB CHRX CT960633, i.e., the *European Pulsar Network*.

## REFERENCES

- Alpar, M. A., Cheng, A. F., Ruderman, M. A., & Shaham, J. 1982, *Nature*, 300, 728
- Arons, J. 1993, *ApJ*, 408, 160
- Arzoumanian, Z., Phillips, J. A., Taylor, J. H., & Wolszczan, A. 1996, *ApJ*, 470, 1111
- Backer, D. C. 1995, *J. Astrophys. Astr.*, 16, 165
- Backer, D. C., Kulkarni, S. R., Heiles, C., Davis, M. M., & Goss, W. M. 1982, *Nature*, 300, 615
- Backer, D. C., Dexter, M. R., Zepka, A., Werthimer, D. J., Ray, P. S., & Foster, R. S. 1997, *PASP*, 109, 61
- Bailes, M., et al. 1994, *ApJ*, 425, L41
- Bailes, M., et al. 1997, *ApJ*, 481, 386
- Bell, J. F., Bailes, M., Manchester, R. N., Lyne, A. G., Camilo, F., & Sandhu, J. S. 1997, *MNRAS*, 286, 463
- Biggs, J. D. 1990, *MNRAS*, 245, 514
- Bhattacharya, D., & van den Heuvel, E. P. J. 1991, *Phys. Rep.*, 203, 1
- Blaskiewicz, M., Cordes, J. M., & Wasserman, I. 1991, *ApJ*, 370, 643
- Boriakoff, V., Buccheri, R., & Fauci, F. 1983, *Nature*, 304, 417
- Camilo, F. 1996, in *Proc. IAU Colloq. 160, Pulsars: Problems & Progress*, ed. S. Johnston, M. Walker, M. Bailes, (San Francisco: PASP), p. 539
- Camilo, F., Nice, D. J., & Taylor, J. H. 1993, *ApJ*, 412, L37
- Camilo, F., Thorsett, S. E., & Kulkarni, S. R. 1994 *ApJ*, 421, L15
- Camilo, F., Nice, D. J., & Taylor, J. H. 1996a, *ApJ*, 461, 812
- Camilo, F., Nice, D. J., Shrauner, J. A., & Taylor, J. H. 1996b, *ApJ*, 469, 819
- Chen, K., & Ruderman, M. 1993, *ApJ*, 408, 179
- Cheng, K. S., Ho, C., & Ruderman, M. 1986, *ApJ*, 300, 500
- Clifton, T. R., Lyne, A. G., Jones, A. W., McKenna, J., & Ashworth, M. 1992, *MNRAS*, 254, 177
- Cordes, J. M. 1978, *ApJ*, 222, 1006
- Cordes, J. M., & Stinebring, D. R. 1984, *ApJ*, 277, L53

- Cordes, J. M., Wasserman, I., & Blaskiewicz, M. 1990, *ApJ*, 349, 546
- D’Amico, N., Bailes, M., Lyne, A. G., Manchester, R. N., Johnston, S., & Fruchter, A. S. 1993, *MNRAS*, 260, L7
- Damour, T., & Taylor, J. H. 1991, *ApJ*, 366, 501
- Doroshenko, O. V., & Kopeikin, S. M. 1995, *MNRAS*, 274, 1029
- Emmering, R. T., & Chevalier, R. A. 1989, *ApJ*, 345, 931
- Foster, R. S., Fairhead, L., & Backer, D. C. 1991, *ApJ*, 378, 687
- Foster, R. S., Wolszczan, A., & Camilo, F. 1993, *ApJ*, 410, L91
- Foster, R. S., Cadwell, B. J., Wolszczan, A., & Anderson, S. B. 1995, *ApJ*, 454, 826
- Fruchter, A. S., Stinebring, D. R., & Taylor, J. H. 1988, *Nature*, 333, 237
- Fruchter, A. S., et al. 1990, *ApJ*, 351, 642
- Geppert, U., & Urpin, V. 1996, *MNRAS*, 278, 471
- Gil, J. A., Gronkowski, P., & Rudnicki, W. 1984, *A&A*, 132, 312
- Gil, J. A., Kijak, J., & Seiradakis, J. H. 1993, *A&A*, 272, 268
- Gil, J. A., & Krawczyk, A. 1997, *MNRAS*, 285, 561
- Goldreich, P., & Julian, W. H. 1969, *ApJ*, 157, 869
- Gould, D. M. 1994, PhD-thesis, University of Manchester
- Hoensbroech, A. von, & Xilouris, K. M. 1997a, *A&A*, 324, 981
- Hoensbroech, A. von, & Xilouris, K. M. 1997b, *A&AS*, 126, 121
- Jahan Miri, M., & Bhattacharya, D. 1994, *MNRAS*, 269, 455
- Johnston, S., Lyne, A. G., Manchester, R. N., Kniffen, D. A., D’Amico, N., Lim, J., & Ashworth, M. 1992, *MNRAS*, 255, 401
- Johnston, S., et al. 1993, *Nature*, 361, 613
- Kanbach, G., et al. 1996, *A&AS*, 120, 461
- Kijak, J., Kramer, M., Wielebinski, R., & Jessner, A. 1997a, *A&A*, 318, L63
- Kijak, J., Kramer, M., Wielebinski, R., & Jessner, A. 1997b, *A&A*, in press

- Kramer, M. 1996, in Proc. IAU Colloq. 160, Pulsars: Problems & Progress, ed. S. Johnston, M. Walker, M. Bailes, (San Francisco: PASP), p. 215
- Kramer, M., Wielebinski, R., Jessner, A., Gil, J. A., & Seiradakis, J. H. 1994, A&AS, 107, 515
- Kramer, M., Doroshenko, O., Jessner, A., Wielebinski, R., Wolszczan, A., Camilo, F., Taylor, J. H., & Xilouris, K. M. 1996, in Proc. IAU Colloq. 160, Pulsars: Problems & Progress, ed. S. Johnston, M. Walker, M. Bailes, (San Francisco: PASP), p. 95
- Kramer, M., Xilouris, K. M., Jessner, A., Wielebinski, R., Lorimer, D. R., & Lyne, A. G. 1997, A&A, 322, 846
- Kramer, M., Xilouris, K. M., Camilo, F., Doroshenko, O., Nice, D. J., Jessner, A., Backer, D.C. 1998, in preparation
- Krolik, J. 1991, ApJ, 373, L69
- Lorimer, D. R. 1994, PhD-thesis, University of Manchester
- Lorimer, D. R., et al. 1995a, ApJ, 439, 933
- Lorimer, D. R., Yates, J. A., Lyne, A. G., & Gould, D. M. 1995b, MNRAS, 273, 411
- Lorimer, D. R., Lyne, A. G., Bailes, M., Manchester, R. N., D’Amico, N., Stapper, B. W., Johnston, S., & Camilo, F. 1996, MNRAS, 283, 1383
- Lundgren, S. C., Zepka, A., & Cordes, J. M. 1995, ApJ, 453, 419
- Lyne, A. G., & Manchester, R. N. 1988, MNRAS, 234, 477
- Lyne, A. G., Biggs, J. D., Brinklow, A., McKenna, J., & Ashworth, M. 1988, Nature, 332, 45
- Lyne, A. G., et al. 1998, MNRAS, in press
- Malofeev, V. M. 1996, in Proc. IAU Colloq. 160, Pulsars: Problems & Progress, ed. S. Johnston, M. Walker, M. Bailes, (San Francisco: PASP), p. 271
- Malofeev, V. M., Gil, J. A., Jessner, A., Malov, I. F., Seiradakis, J. H., Sieber, W., & Wielebinski, R. 1994, A&A, 285, 201
- Manchester, R. N. 1992, in Proc. of IAU Colloq. 128, ed. T. Hankins, J.M. Rankin, J. A. Gil, (Zielona Gora: Pedagogical University Press), p. 206
- Manchester, R. N., & Taylor, J. H. 1977, Pulsars, (San Francisco: Freeman)
- Manchester, R. N., & Johnston, S. 1995, ApJ, 441, L65
- Manchester, R. N., et al. 1996, MNRAS, 279, 1235



- Matese, J. J., & Whitmire, D. P. 1980, *ApJ*, 235, 587
- Melrose, D. B. 1992, *Phil. Trans. Roy. Soc. Lond.*, A341, 105
- Narayan, R., & Vivekanand, M. 1983, *A&A*, 122, 45
- Navarro, J., de Bruyn, A. G., Frail, D. A., Kulkarni, S. R., & Lyne, A. G. 1995, *ApJ*, 455, L55
- Navarro, J., & Manchester, R. N. 1996, *Proc. IAU Colloq. 160, Pulsars: Problems & Progress*, eds. S. Johnston, M. Walker, M. Bailes, *PASP*, p. 249
- Nicastro, L., Lyne, A. G., Lorimer, D. R., Harrison, P. A., Bailes, M., & Skidmore, B. D. 1995, *MNRAS*, 273, L68
- Nice, D. J. 1992, PhD-thesis, Princeton University
- Nice, D. J., Taylor, J. H., & Fruchter, A. S. 1993, *ApJ*, 402, L49
- Nice, D. J., & Taylor, J. H. 1995, *ApJ*, 441, 429
- Nice, D. J., Sayer, R. W., & Taylor, J. H. 1996, *ApJ*, 466, L87
- Ott, M., Witzel, A., Quirrenbach, A., Krichbaum, T. P., Standke, K. J., Schalinski, C. J., & Hummel, C. A. 1994, *A&A*, 284, 331
- Phillips, J. A. 1992, *ApJ*, 385, 282
- Phillips, J. A., & Wolszczan, A. 1992, *ApJ*, 385, 273
- Phinney, E. S., & Kulkarni, S. R. 1994, *ARA&A*, 32, 591
- Radhakrishnan, V., & Cooke, D. J. 1969, *Astrophys. Lett.*, 3, 225
- Rankin, J. M. 1983, *ApJ*, 274, 333
- Rankin, J. M. 1990, *ApJ*, 352, 247
- Rankin, J. M. 1993a, *ApJ*, 405, 285
- Rankin, J. M. 1993b, *ApJS*, 85, 145
- Romani, R. W. 1990, *Nature*, 347, 741
- Ruderman, M. 1991, *ApJ*, 382, 576
- Ruderman, M. A., & Sutherland, P. G. 1975, *ApJ*, 196, 51
- Sayer, R. W., Nice, D. J., & Taylor, J. H. 1997, *ApJ*, 474, 426

- Segelstein, D. J., Rawley, L. A., Stinebring, D. R., Fruchter, A. S., & Taylor, J. H. 1986, *Nature*, 322, 714
- Seiradakis, J. H., Gil, J. A., Graham, D. A., Jessner, A., Kramer, M., Malofeev, V. M., Sieber, W., & Wielebinski, R. 1995, *A&AS*, 111, 205
- Shklovskii, I. S. 1970, *Sov. Astron.*, 13, 562
- Srinivasan, G., Bhattacharya, D., Muslimov, A. G., & Tsygan, A. I. 1990, *Curr. Sci.*, 59, 31
- Stappers, B. W., et al. 1996, *ApJ*, 465, L119
- Taylor, J. H., & Weisberg, J. M. 1982, *ApJ*, 253, 908
- Taylor, J. H., & Weisberg, J. M. 1989, *ApJ*, 345, 434
- Taylor, J. H., & Cordes, J. M. 1993, *ApJ*, 411, 674
- Taylor, J. H., Manchester, R., & Lyne, A.G. 1993, *ApJS*, 88, 529
- Taylor, J.H., Manchester, R. N., Lyne, A. G., & Camilo, F. 1995, unpublished (available at <ftp://pulsar.princeton.edu/pub/catalog>)
- Thorsett, S. E., & Stinebring, D. R. 1990, *ApJ*, 361, 644
- Van den Heuvel, E. P. J., & Bitzaraki, O. 1995, *A&A*, 297, L41
- Wolszczan, A. 1991, *Nature*, 350, 688
- Wolszczan, A. 1996, in *Proc. IAU Colloq. 160, Sydney 1996: Pulsars: Problems & Progress*, ed. S. Johnston, M. Walker, M. Bailes, (San Francisco: PASP), p. 91
- Wolszczan, A., & Frail, D. A. 1992 *Nature*, 355, 145
- Xilouris, K. M., Kramer, M., Jessner, A., Wielebinski, R., & Timofeev, M. 1996, *A&A*, 309, 481
- Xilouris, K. M., Kramer, M., Jessner, A., Hoensbroech, A. v., Lorimer, D. R., Wielebinski, R., Wolszczan, A., & Camilo, F. 1998a, *ApJ*, in press (paper II)
- Xilouris, K. M., Kramer, M., Hoensbroech, A. v. 1998b, in preparation (paper III)

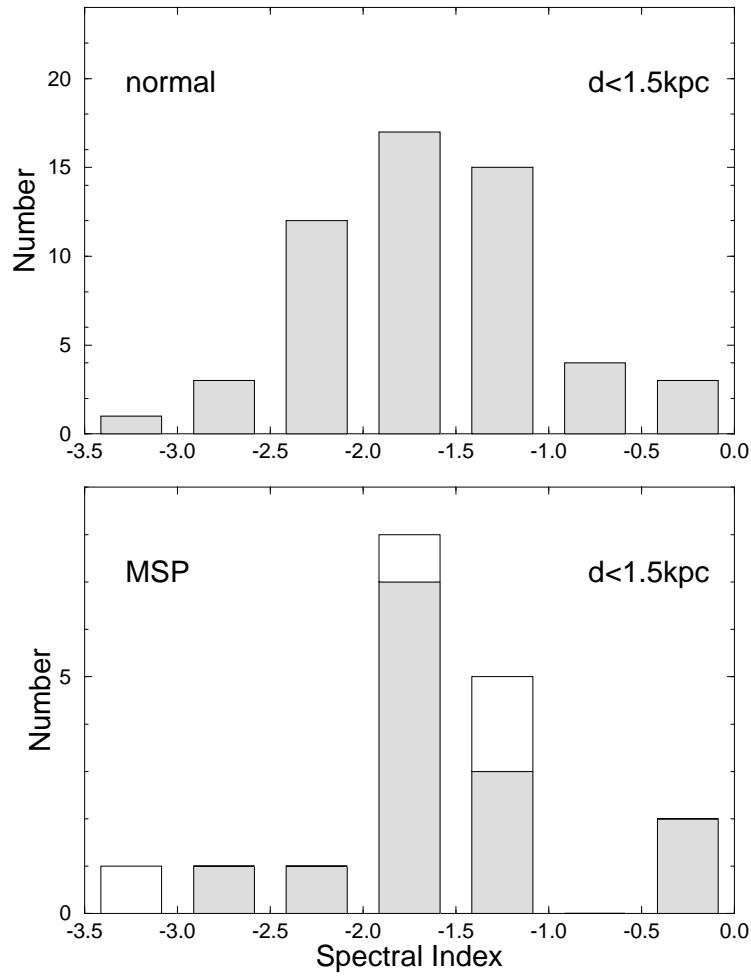


Fig. 1.— Distribution of spectral indices for normal and millisecond pulsars within a distance of 1.5 kpc. Data for MSPs indicated by unshaded bars are derived from the literature (see text for details).

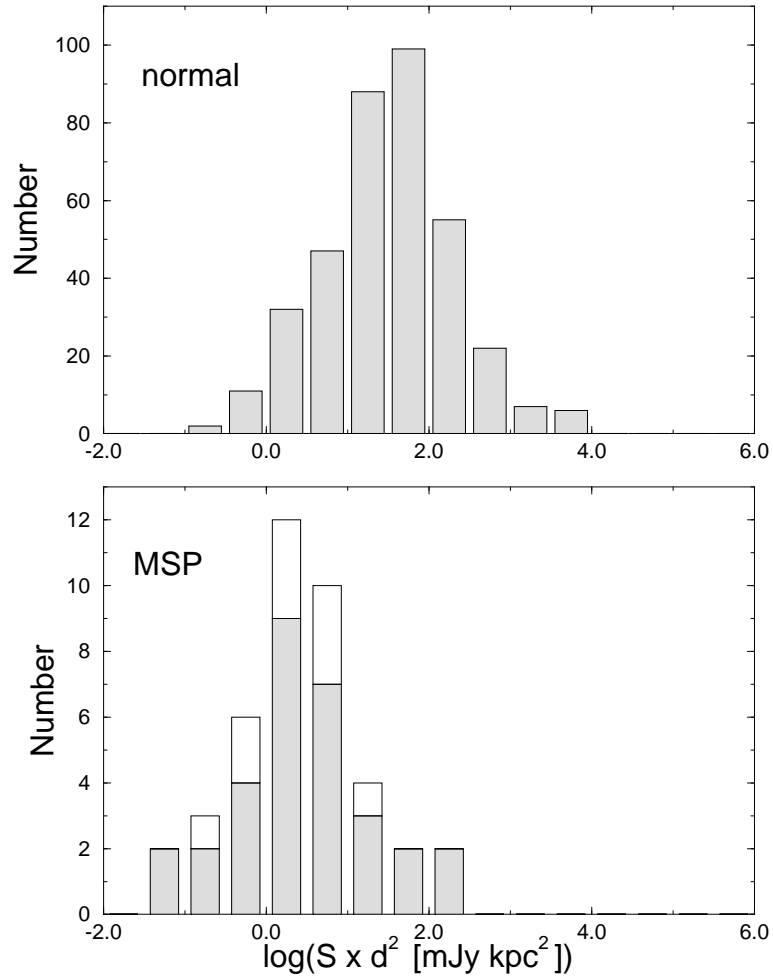


Fig. 2.— Luminosity distribution derived for normal and millisecond pulsars. Data for MSPs indicated by unshaded bars are taken from the literature (see text for details).

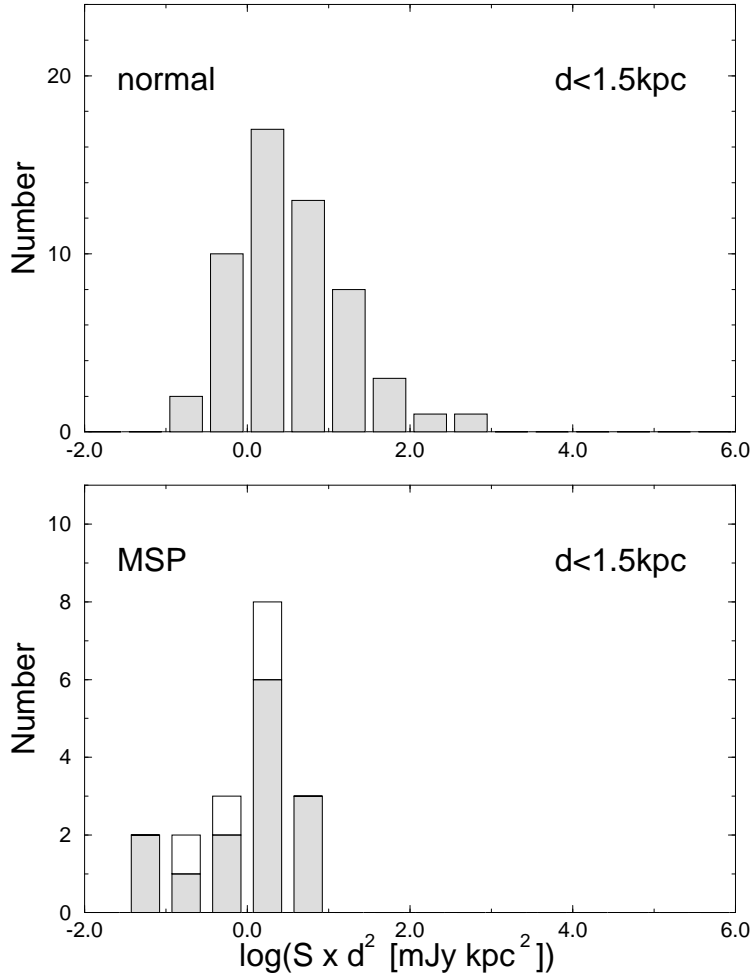


Fig. 3.— Luminosity distribution derived for sources within a distance of 1.5 kpc. Data for MSPs indicated by unshaded bars are derived from the literature (see text for details). We note that there seems to be a particular deficit in the number of high-luminosity MSPs relative to the normal pulsars.

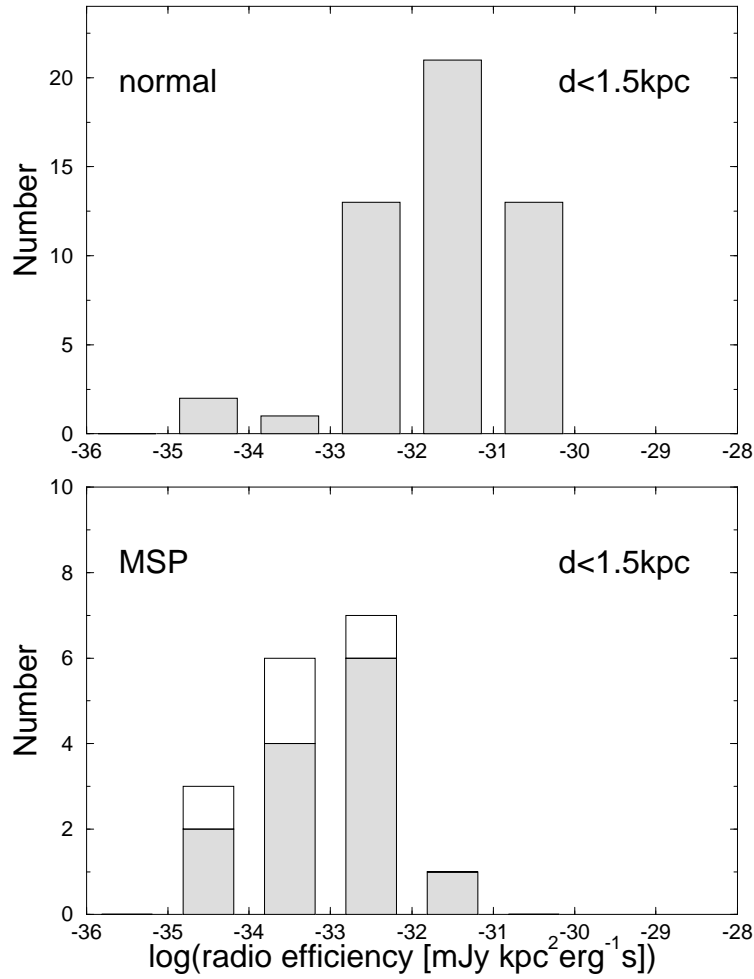


Fig. 4.— Comparison of the efficiency of normal and millisecond pulsars as radio sources. Only those objects located within a distance of 1.5 kpc are considered. Data for MSPs indicated by unshaded bars are derived from the literature (see text for details).

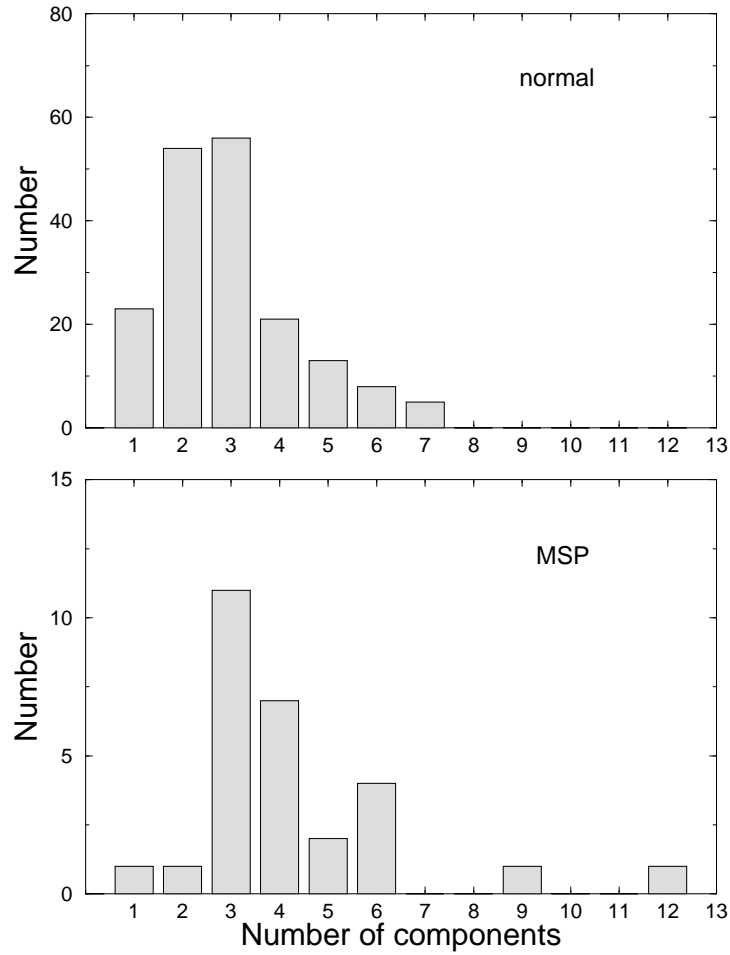


Fig. 5.— Complexity of profiles for normal and millisecond pulsars as expressed by number of components in each profile.

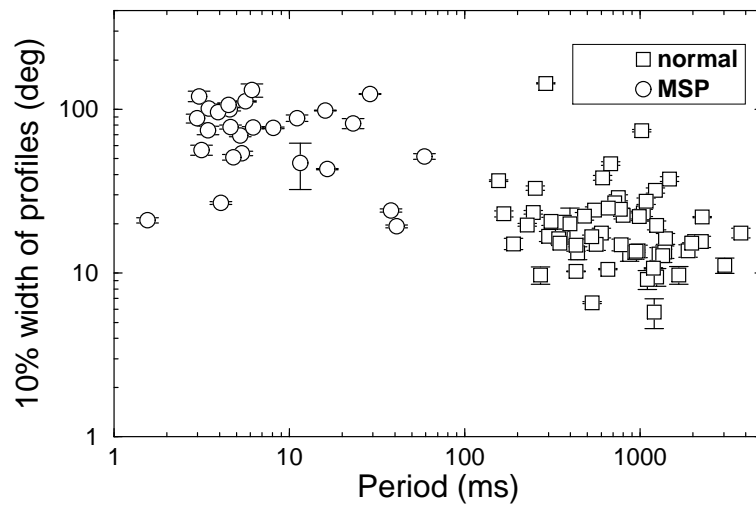


Fig. 6.— Profile width measured at a 10% intensity level for normal pulsars (squares) and MSPs (circles) as a function of pulse period.

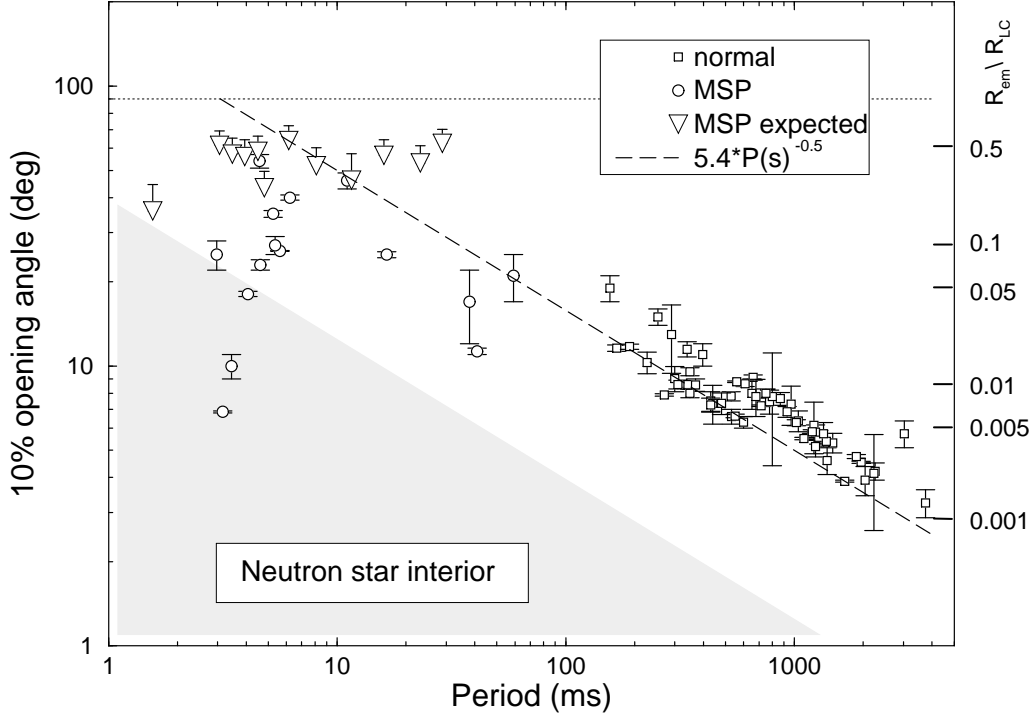


Fig. 7.— Opening angles derived for a 10% intensity level for normal pulsars (squares) and MSPs (circles) as a function of pulse period. For normal pulsars, the opening angles scale with  $P^{-0.5}$  as indicated by the dashed line derived by Gould (1994). MSPs seem not to follow the same scaling, which is supported by the determined upper limits also presented. The triangles mark the expectation value,  $\langle \rho \rangle$ , while the upper bar indicates an upper limit valid with 68% probability (see text for details). Assuming dipolar magnetic field lines, we have marked the region of opening angles which corresponds to the interior of a neutron star of 10 km radius. With the same assumption one can translate an opening angle into an emission height in units of fraction of the light cylinder. A corresponding scale is indicated on the right border of the plot. The maximum possible value of the opening angle of  $90^\circ$  is marked by a dotted line.



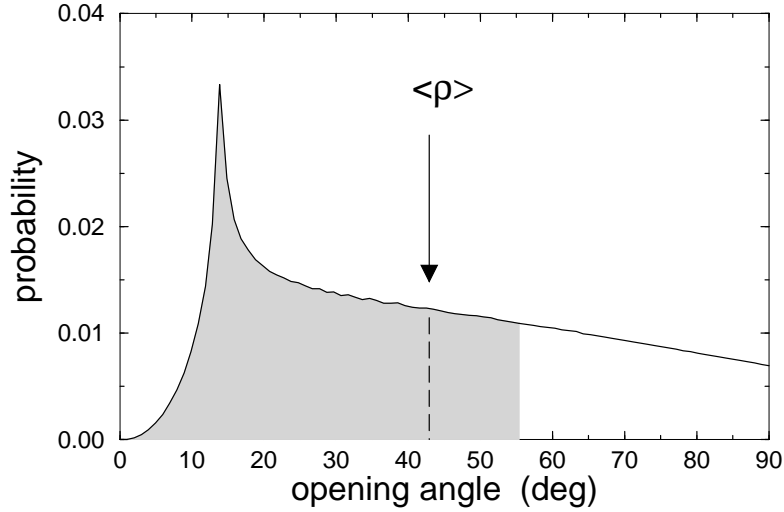


Fig. 8.— Probability distribution for the occurrence of values for the opening angle  $\rho$  derived for J1744–1134 with a 10%-profile width of  $26.8^\circ$ . For this case, the most likely value of  $\rho$  given by the peak of the probability function is  $13.8^\circ$ . The expectation value  $\langle \rho \rangle$  is marked at  $42.2^\circ$ . With a probability of 68% the true value of  $\rho$  is smaller than  $55.4^\circ$  (shaded area). These values are to be compared to an opening angle derived from polarisation measurements of  $18.1^\circ$ .

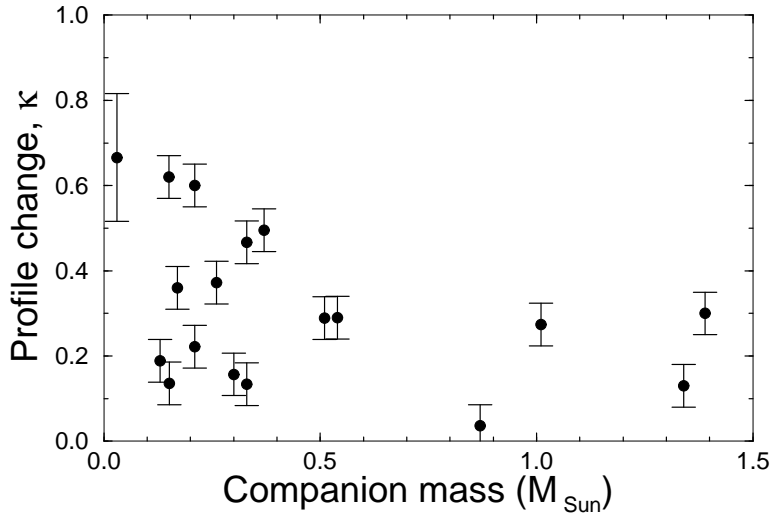


Fig. 9.— Parameter describing the profile development between 400 MHz and 1400 MHz (for definition see text) as a function of companion mass.

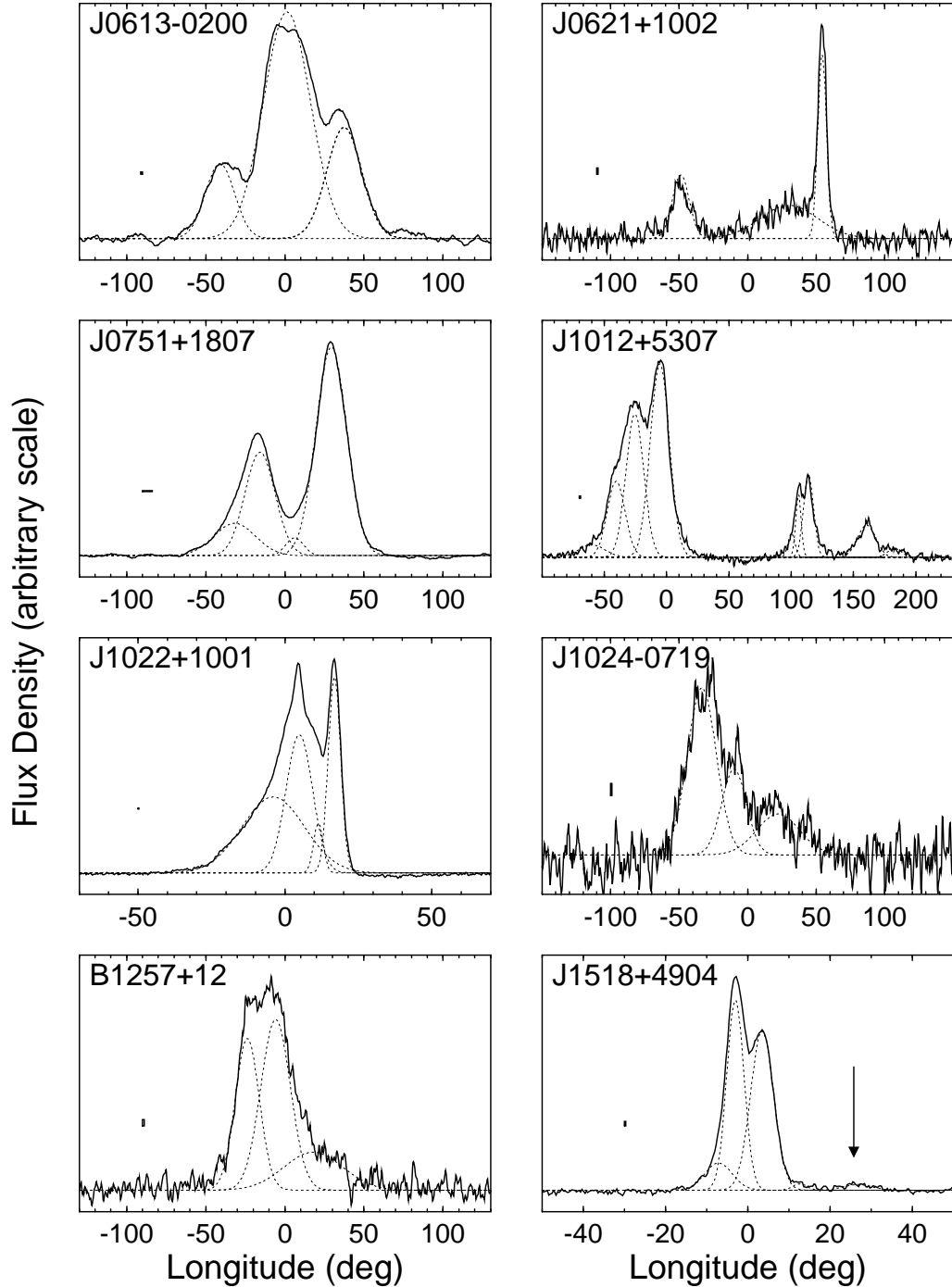


Fig. 10.— Average pulse profiles for eight MSPs at a frequency of 1.4 GHz. The root mean square (RMS) measured in an off-pulse region is indicated by the height of the small box left of the pulse. Its width indicates the resolution of the profile (see text for details). Residuals obtained from fitting Gaussian components (dashed lines) to the profiles are not plotted for clarity. The arrow shown in the profile of J1518+4904 points toward a detected post-cursor.

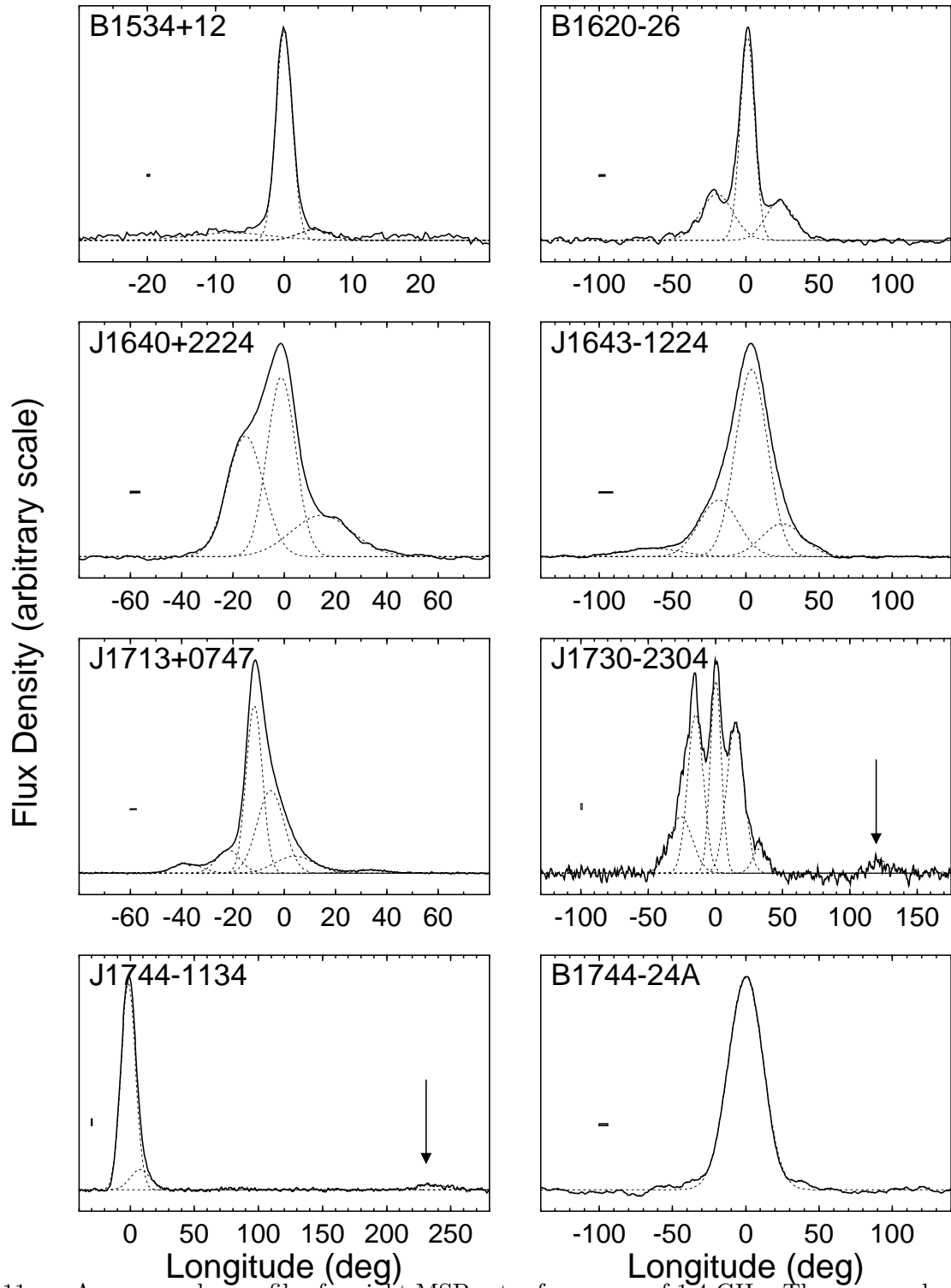


Fig. 11.— Average pulse profiles for eight MSPs at a frequency of 1.4 GHz. The arrows shown for J1730–2304 and J1744–1134 point toward detected post-cursor and pre-cursor, respectively.

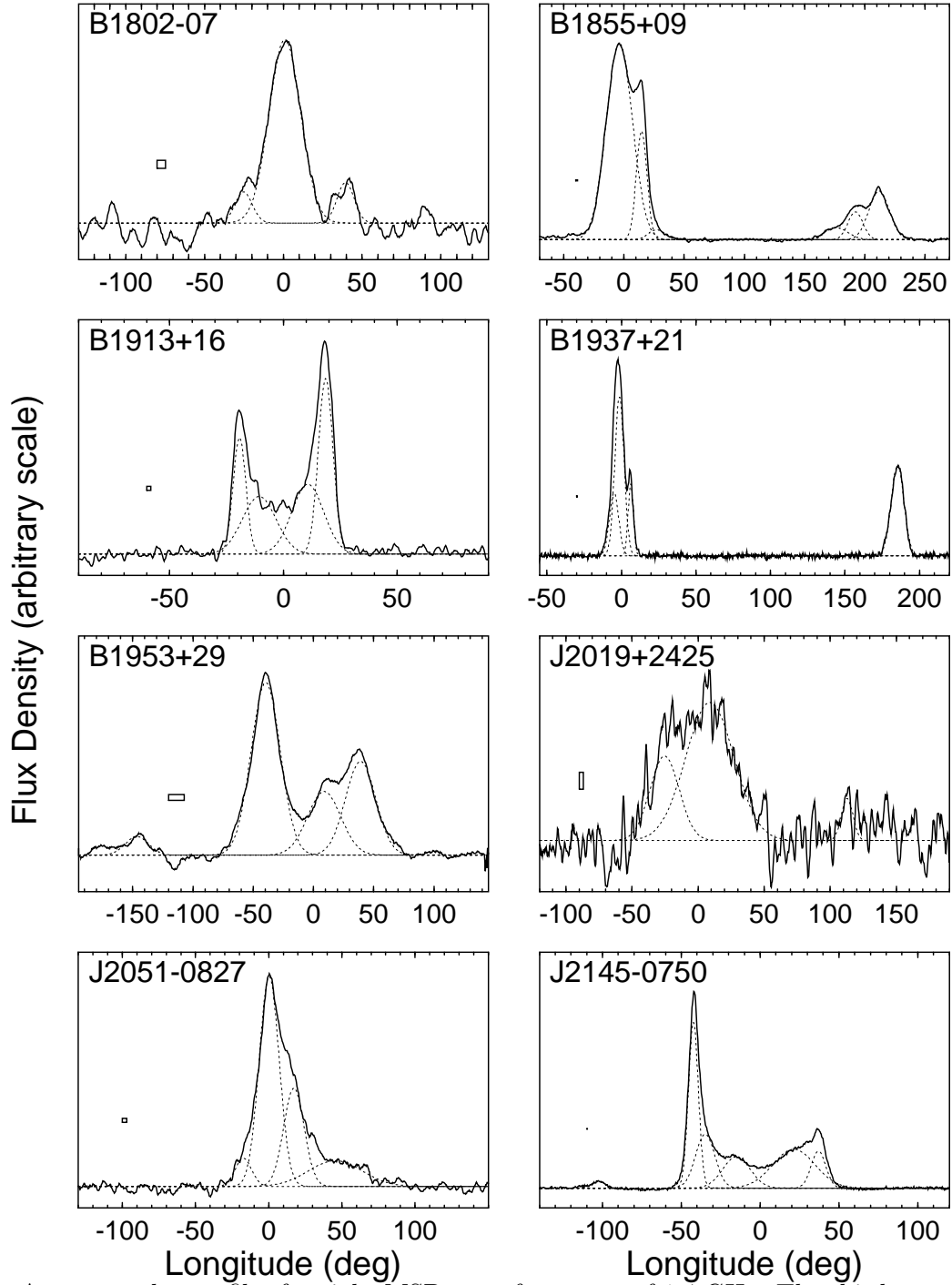


Fig. 12.— Average pulse profiles for eight MSPs at a frequency of 1.4 GHz. The third component tentatively fitted to the low signal-to-noise-ratio profile of J2019+2425 at about  $104^\circ$  corresponds to component *D* seen by Nice(1992).

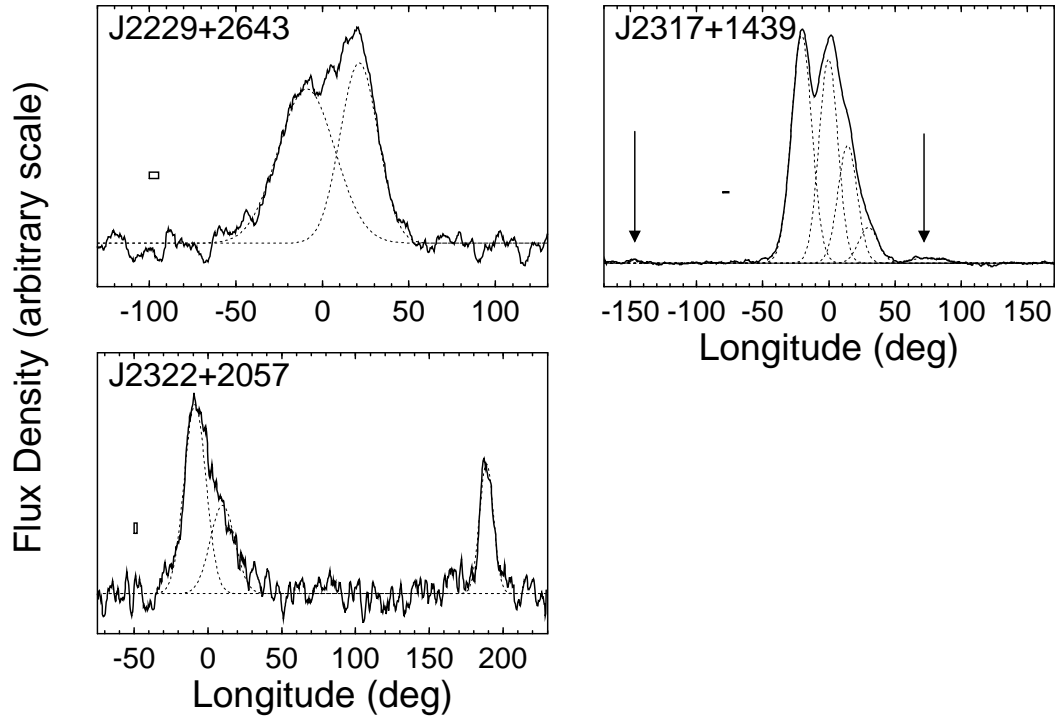


Fig. 13.— Average pulse profiles for eight MSPs at a frequency of 1.4 GHz. The arrows shown for J2317+1439 point toward a detected pre- and post-cursor of the pulse.

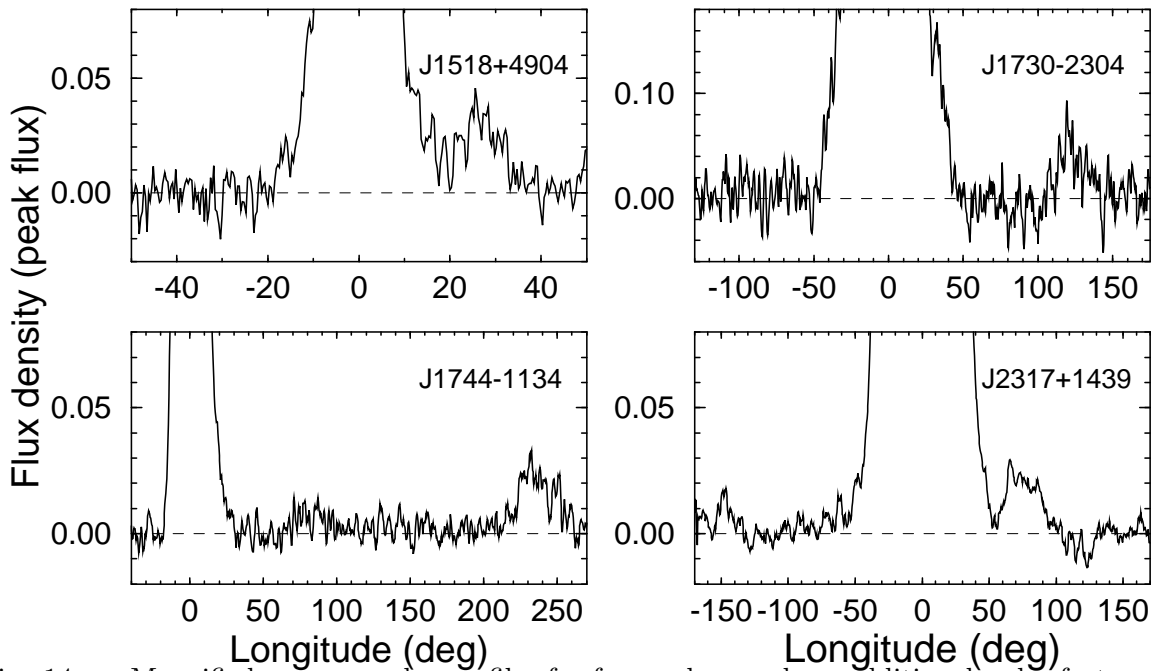


Fig. 14.— Magnified average pulse profiles for four pulsars, where additional pulse features have been detected.

Table 1. Flux densities and spectral indices for 34 millisecond pulsars. The flux density data presented for the first 23 sources were derived from our measurements, while for 11 sources we collected data from the literature. Besides the period of the pulsar (column 2), we quote the corresponding frequency in column 3. The mean flux density and its uncertainty is shown in column 4. Additionally, we present the median of all measured flux values, which is to be compared with the mean value. The spectral index is derived by using published lower frequency data (for references see column 7) which is indicated in column 6.

PSR	P (ms)	$\nu_{\text{eff}}$ (GHz)	$S_{\text{mean}}$ (mJy)	$S_{\text{median}}$ (mJy)	spectral index $\alpha$	Ref.
J0613–0200	3.062	1.410	1.4 ± 0.2	1.5	–1.9 ± 0.4	1
J0751+1807	3.479	1.435	3.2 ± 0.7	2.9	–0.9 ± 0.3	2
J1012+5307	5.256	1.410	3 ± 1	1.9	–1.8 ± 0.4	3
J1022+1001	16.453	1.443	3.0 ± 0.4	2.5	–1.7 ± 0.1	4, 5
J1024–0719	5.162	1.410	0.66 ± 0.04	0.66	–1.5 ± 0.2	6
B1257+12	6.219	1.410	2 ± 1	2	–1.9 ± 0.5	7
J1518+4904	40.935	1.410	4 ± 2	2.5	–0.5 ± 0.5	26, 30
B1534+12	37.904	1.530	0.6 ± 0.2	0.4	–3.0 ± 0.4	8
B1620–26	11.076	1.460	1.6 ± 0.3	1.7	–2.5 ± 0.2	9, 10
J1640+2224	3.163	1.472	2 ± 1	1	–0.3 ± 0.5	11
J1643–1224	4.621	1.410	4.8 ± 0.6	4.5	–2.4 ± 0.3	1
J1713+0747	4.570	1.510	8 ± 2	5	–1.5 ± 0.1	12
J1730–2304	8.123	1.410	4 ± 3	2	–1.8 ± 0.3	1
J1744–1134	4.075	1.470	3 ± 1	2	–1.6 ± 0.3	6
B1802–07	23.101	1.410	1.0 ± 0.5	1.0	–1.0 ± 0.5	13
B1855+09	5.362	1.470	5 ± 1	4	–1.3 ± 0.2	10, 14
B1913+16	59.030	1.560	0.9 ± 0.2	0.9	–1.4 ± 0.3	15, 27
B1937+21	1.558	1.579	10 ± 1	9	–2.3 ± 0.2	10
B1953+29	6.133	1.410	1.1 ± 0.2	1.1	–2.2 ± 0.3	16
J2051–0827	4.509	1.410	2.8 ± 0.6	2.5	–1.8 ± 0.3	17
J2145–0750	16.052	1.510	8 ± 2	7	–1.6 ± 0.1	18
J2229+2643	2.978	1.430	0.9 ± 0.2	0.8	–2.2 ± 0.5	19
J2317+1439	3.445	1.496	4 ± 1	2	–1.4 ± 0.3	20
J0218+4232	2.323	1.410	0.9 ± 0.2	–	–2.8 ± 0.2	21
J0437–4715	5.757	1.460	142 ± 53	–	–1.8 ± 0.2	22, 23
J0621+1002	28.853	0.800	1.9 ± 0.3	–	–2.5 ± 1.4	4
J0711–6830	5.491	1.400	1.6 ± 0.3	–	–1.4 ± 0.2	6
J1045–4509	7.474	1.520	3 ± 1	–	–1.5 ± 0.3	18
J1603–7202	14.841	1.400	3.0 ± 0.5	–	–1.3 ± 0.3	24
J1804–2717	9.343	1.400	0.4 ± 0.2	–	–3.2 ± 0.5	24
J1911–1114	3.625	1.400	0.5 ± 0.2	–	–3.3 ± 0.4	24
B1957+20	1.607	1.400	0.4 ± 0.2	–	–3.5 ± 0.5	25, 30
J2124–3358	4.931	1.400	1.6 ± 0.4	–	–1.1 ± 0.4	6
J2129–5721	3.726	1.400	1.4 ± 0.2	–	–1.0 ± 0.4	24

Table 2. Pulse widths measured for millisecond pulsars. Besides the period of each pulsar (column 2) we quote the width at a 50% and 10% level and their corresponding uncertainty in degrees (columns 3 – 6), and in units of time (columns 7 – 10). We used the 10% width to derive a duty cycle quoted in column 11.

PSR	P (ms)	$W_{50}$ (deg)	$W_{10}$ (deg)	$W_{\text{eq}}$ (deg)	$\Delta W$ (deg)	$W_{50}$ (ms)	$W_{10}$ (ms)	$W_{\text{eq}}$ (ms)	$\Delta W$ (ms)	10% Duty Cycle (%)
J0613–0200	3.062	101	120	58	9	0.86	1.02	0.49	0.08	33 ± 3
J0621+1002	28.854	114.2	124.0	20.9	0.9	9.15	9.94	1.68	0.07	34.4 ± 0.3
J0751+1807	3.479	73	101	42	6	0.70	0.98	0.40	0.06	28 ± 2
J1012+5307	5.256	47	69	41	1	0.69	1.01	0.59	0.02	19.2 ± 0.3
J1022+1001	16.453	23.3	43.2	22.8	0.4	1.07	1.97	1.04	0.02	12.0 ± 0.1
J1024–0719	5.612	41.1	111.9	46.8	0.9	0.59	1.60	0.67	0.01	31.1 ± 0.3
B1257+12	6.219	38	77	44	1	0.66	1.34	0.75	0.02	21.5 ± 0.3
J1518+4904	40.935	12.5	19.3	11.1	0.6	1.42	2.19	1.26	0.07	5.4 ± 0.2
B1534+12	37.904	2.9	24.1	3.7	0.6	0.31	2.54	0.39	0.06	6.7 ± 0.2
B1620–26	11.076	67	88	22	4	2.1	2.7	0.7	0.1	25 ± 1
J1640+2224	3.163	25	56	27	4	0.22	0.50	0.24	0.04	16 ± 1
J1643–1224	4.621	32	78	41	2	0.41	1.00	0.52	0.03	21.6 ± 0.6
J1713+0747	4.570	11	100	15	3	0.14	1.27	0.19	0.03	27.8 ± 0.7
J1730–2304	8.123	47.4	77.0	39.1	0.9	1.07	1.73	0.88	0.02	21.4 ± 0.3
J1744–1134	4.075	13.8	26.8	15.2	0.6	0.156	0.303	0.172	0.007	7.4 ± 0.2
B1744–24A	11.564	26	47	28	15	0.8	1.5	0.9	0.5	13 ± 4
B1802–07	23.101	57	82	30	6	3.7	5.3	1.9	0.4	23 ± 2
B1855+09	5.362	36	54	34	2	0.54	0.80	0.51	0.03	14.9 ± 0.5
B1913+16	59.030	45	52	21	2	7.4	8.5	3.5	0.3	14.3 ± 0.6
B1937+21 <sup>a</sup>	1.558	14.6	20.0	10.5	0.2	0.063	0.087	0.045	0.001	5.55 ± 0.06
B1953+29	6.133	107	131	60	12	1.8	2.2	1.0	0.2	36 ± 3
J2019+2425	3.935	67	96	62	3	0.73	1.05	0.68	0.03	26.7 ± 0.8
J2051–0827	4.509	27	107	32	3	0.34	1.33	0.40	0.04	29.6 ± 0.9
J2145–0750	16.052	88.6	98.4	23.6	0.4	3.95	4.39	1.05	0.02	27.3 ± 0.1
J2229+2643	2.978	70	88	53	6	0.58	0.73	0.44	0.05	24 ± 2
J2317+1439	3.445	48	74	48	5	0.46	0.71	0.45	0.04	21 ± 1
J2322+2057	4.808	23	51	27	2	0.30	0.68	0.36	0.03	14.2 ± 0.6

<sup>a</sup>width measured from EBPP data (see text for details)

Table 3. Opening angles for MSPs derived from profile widths measured at 10% intensity level. Calculations are based on fits of the rotating-vector-model to polarisation data to derive the viewing geometry (paper IV). In cases where this is not possible, we quote values expected from statistical arguments,  $\langle \rho_{10} \rangle$  (see text for details).

PSR	P (ms)	$\rho_{10}$ (deg)	$\langle \rho_{10} \rangle$ (deg)
J0613–0200	3.062	–	61.5
J0621+1002	28.854	–	62.4
J0751+1807	3.479	–	57.2
J1012+5307	5.256	35 ± 1	–
J1022+1001	16.453	25.0 ± 0.6	–
J1024–0719	5.612	25.8 ± 0.1	–
B1257+12	6.219	40.0 ± 0.9	–
J1518+4904	40.935	10.5 ± 0.4	–
B1534+12 <sup>a</sup>	37.904	17 ± 5	–
B1620–26	11.076	46 ± 3	–
J1640+2224	3.163	6.9 ± 0.1	–
J1643–1224	4.621	23 ± 1	–
J1713+0747	4.570	54 ± 3	–
J1730–2304	8.123	–	52.0
J1744–1134	4.075	18.1 ± 0.4	–
B1744–24A	11.564	–	46.1
B1802–07	23.101	–	53.1
B1855+09	5.362	27 ± 2	–
B1913+16 <sup>b</sup>	59.030	21 ± 4	–
B1937+21	1.558	–	35.8
B1953+29	6.133	–	63.9
J2019+2425	3.935	–	56.1
J2051–0827	4.509	–	58.6
J2145–0750	16.052	–	56.7
J2229+2643	2.978	25 ± 3	–
J2317+1439	3.445	10 ± 1	–
J2322+2057	4.808	–	43.3

<sup>a</sup>using viewing geometry derived by Arzoumanian et al. (1996)

<sup>b</sup>using viewing geometry constrained by Cordes et al. (1990)